Laser absorption in plasmas: from nano-targets to near-QED regime

HEINRICH HEINE
UNIVERSITÄT DÜSSELDORF

A. Pukhov, V.Kaymak, D. Zhu, Z.Y. Chen, HHUD, Germany

B.F.Shen, SIOM, China

I. Kostyukov, E. Nerush IAP RAS, Russia

J.Rocca, V. Shlyaptsev, M. Purvis CSU, U.S.A.

L. Ji, K. Akli, OSU, U.S.A.

T.P.Yu, X.L.Zhu, B.Shao NUDT Changsha, China

Z.M.Sheng, Jiao Tong University, China

Nonlinear Waves 2016

Посвящается светлой памяти Н.Б.Нарожного

NW2008

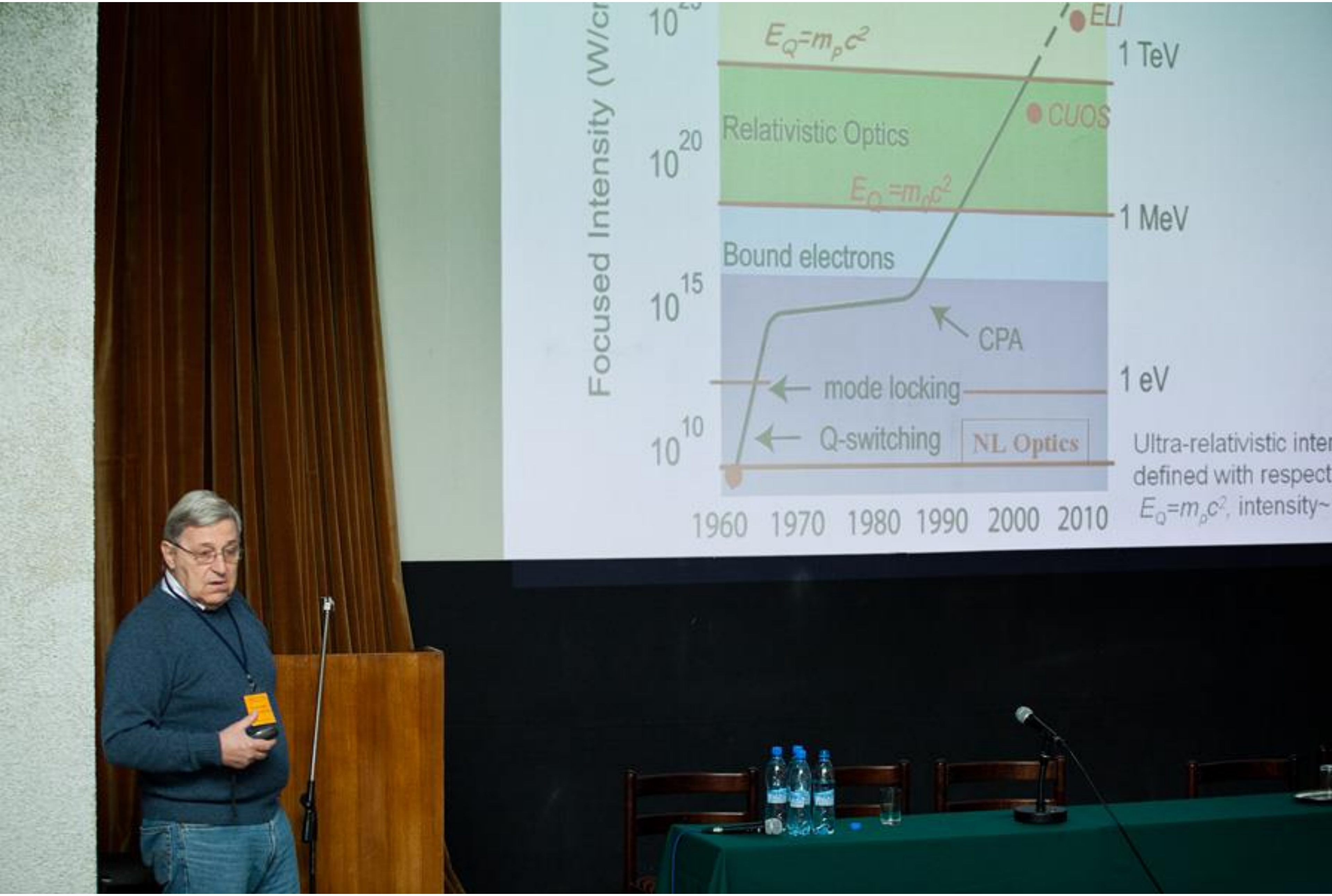

ELI
$E_Q=m_pc^2$
1 TeV
CUOS
Relativistic Optics
10^{20}
$E_Q=m_0c^2$
1 MeV
Bound electrons
10^{15}
CPA
1 eV
mode locking
Q-switching
NL Optics
10^{10}
1960 1970 1980 1990 2000 2010


Focused
10^{15}
10^{10}

Outline

- **Near Critical Density (NCD) plasma**
- **Nanostructured targets:**
  - relativistic plasma nano-photonics
- **Ion acceleration**
- **QED effects**
  - γ-emission, radiation damping, pairs
- **Energy conversion channels**
- **Radiative trapping of electrons**

Non-linear optics in relativistic plasma

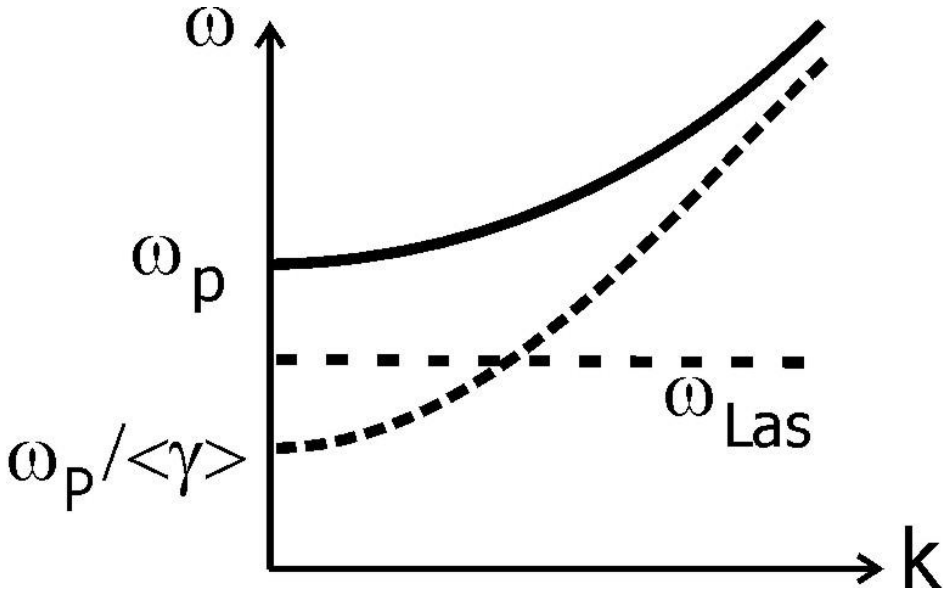

Dispersion of light in plasma:

$$\omega^2 = \omega_p{}^2 + c^2k^2$$

Plasma frequency:

$$\omega_p{}^2 = 4\pi e^2\, n_e\, /(m\langle\gamma\rangle)$$

Relativistic factor:

$$\gamma = (1 - v^2/c^2)^{-1/2}$$

Index of refraction:

$$n_R = (1 - \omega_p{}^2/\ \omega^2)^{1/2}$$

Relativistic self-focussing of laser in plasmas

$\omega_p^2 = 4\pi e^2 n_e / m\gamma_{eff}$

$$n = \sqrt{1 - \omega_p^2 / \omega_L^2}$$

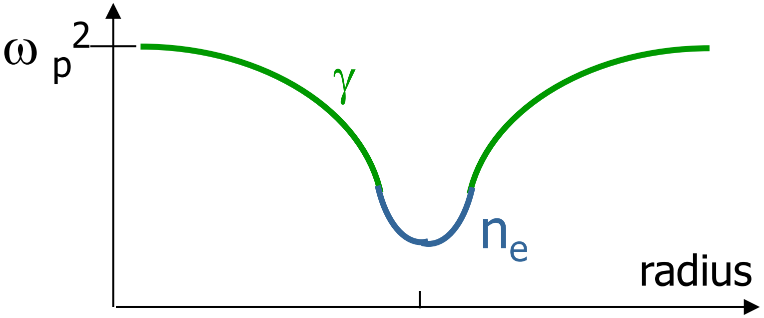

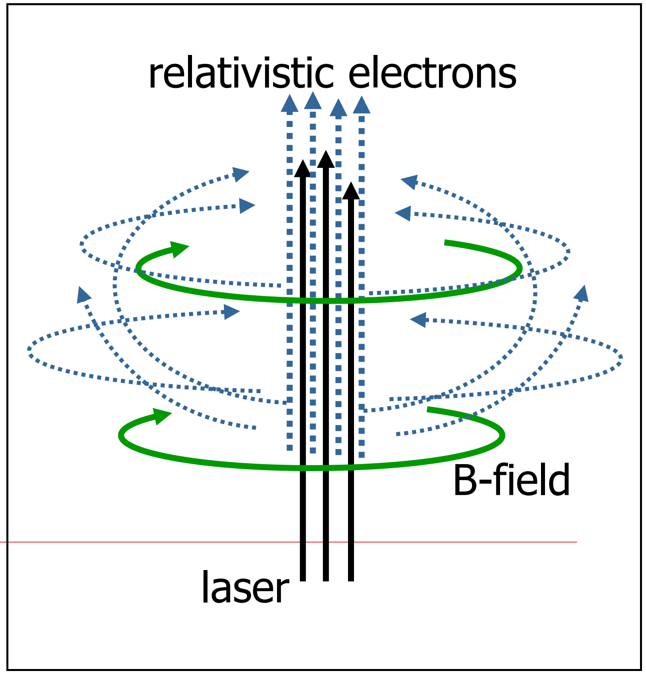

Relativistic mass increase (γ)
and electron density depletion (n_e)
enhance index of refraction in the channel region, leading to self-focussing

Relativistic laser self-channeling in Near Critical Density plasmas

Pukhov, Meyer-ter-Vehn, PRL 76, 3975 (1996)

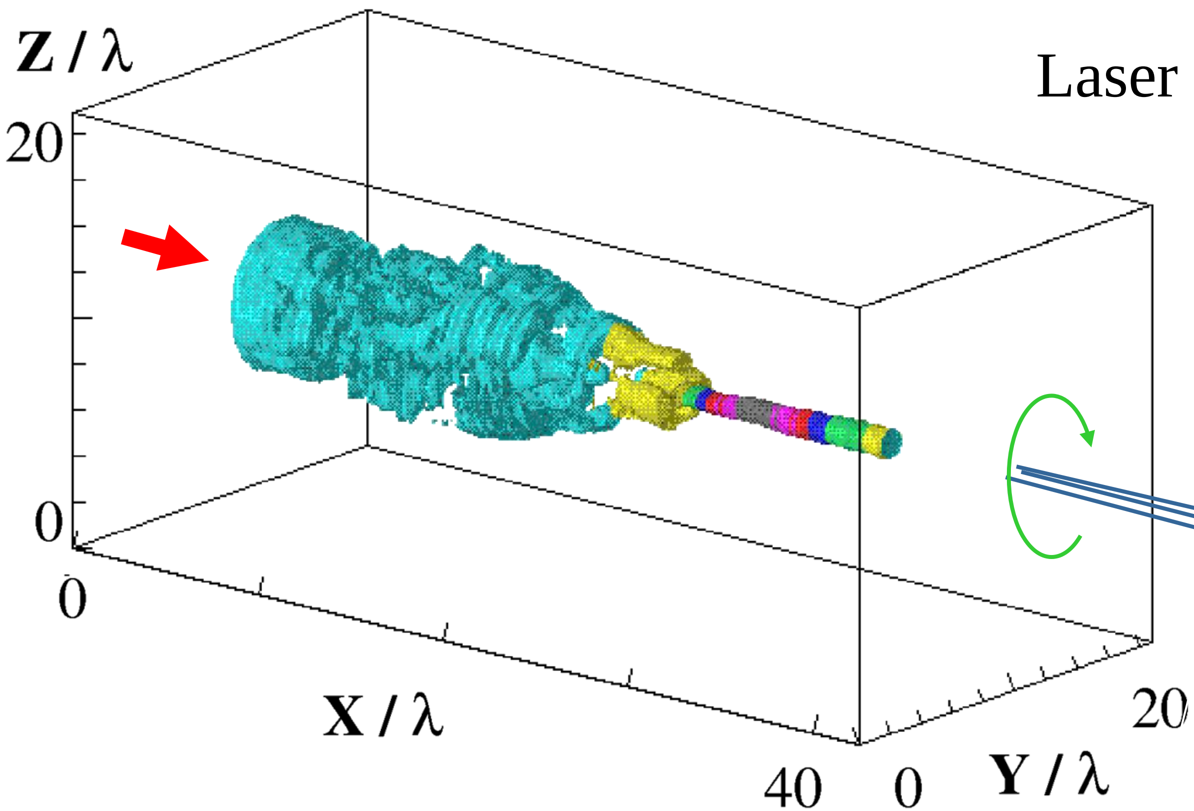

Laser pulse, $I = 10^{19}$ W/cm^2.

$B \sim mc\omega_p/e \sim 10^8$ Gauss

Relativistic electron beam

$j \sim en_c c \sim 10^{12}$ A/cm^2

10 kA of 1-20 MeV electrons

HEINRICH HEINE
UNIVERSITÄT DÜSSELDORF

Explosion of the ion channel

A.Pukhov et al., Phys. Plasmas **6**, p.2847 (1999).

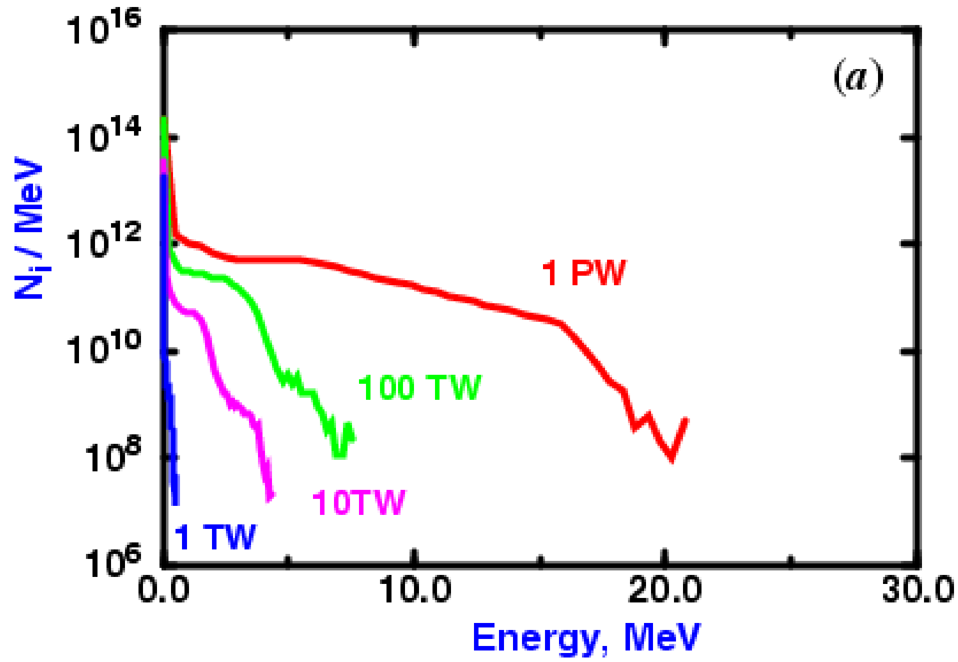

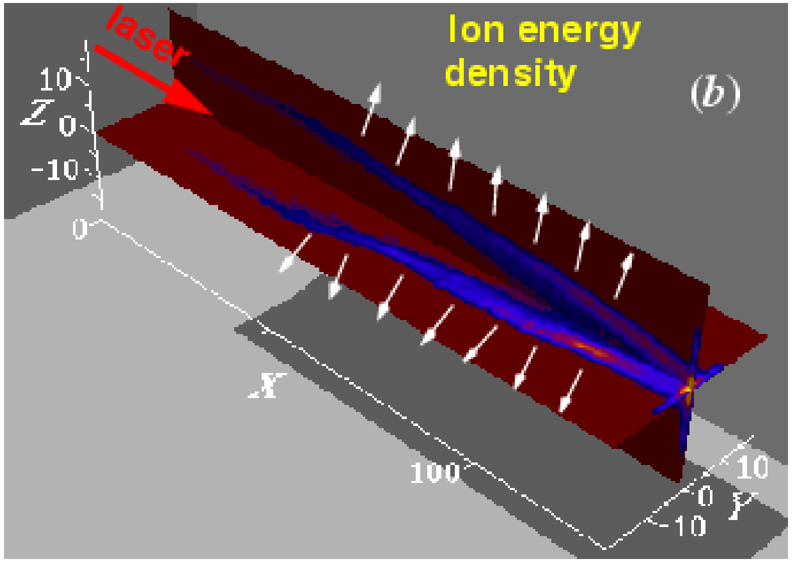

Channel expansion: Strong cylindrical blast wave

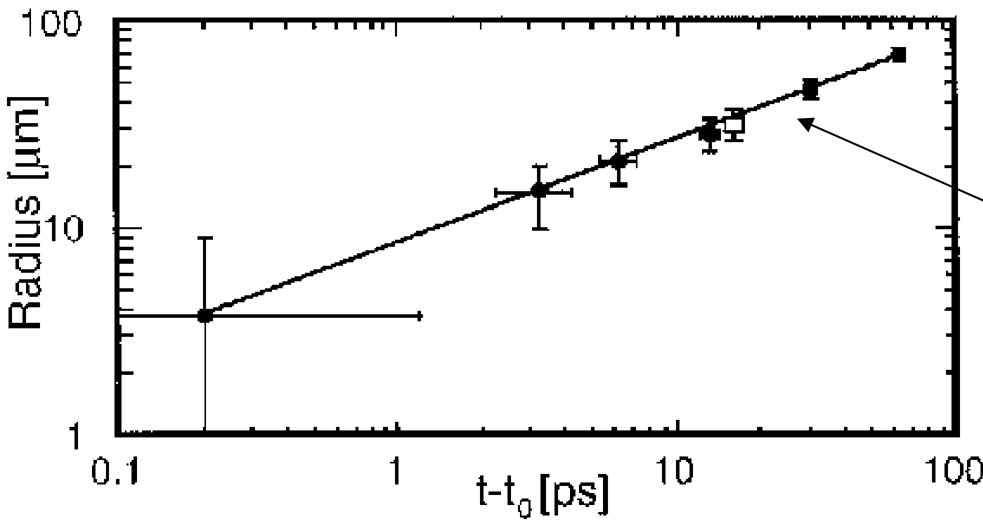

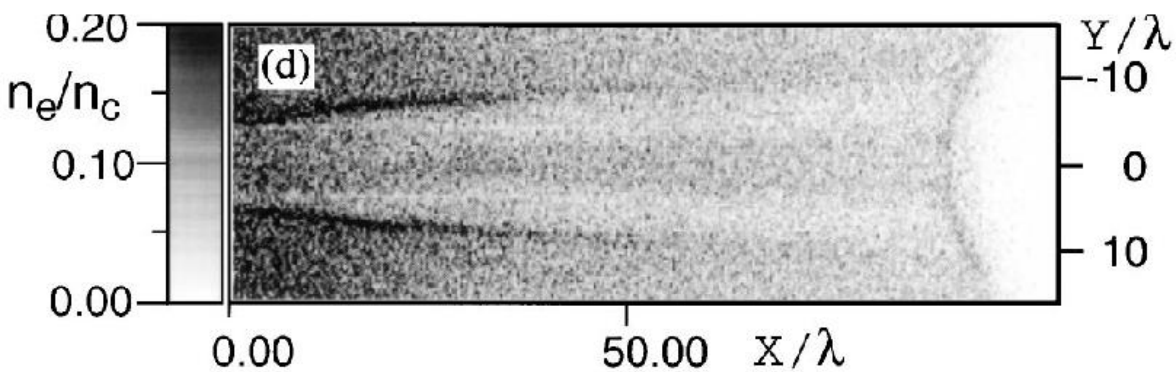

M.Borghesi et al.
PRL **80**, p.5137 (1998).

$$R \sim \sqrt{t}$$

Strong shock scaling cylindrical blast wave

Ion acceleration from solid targets

A.Pukhov, Phys. Rev. Lett. **86**, p.3562 (2001).

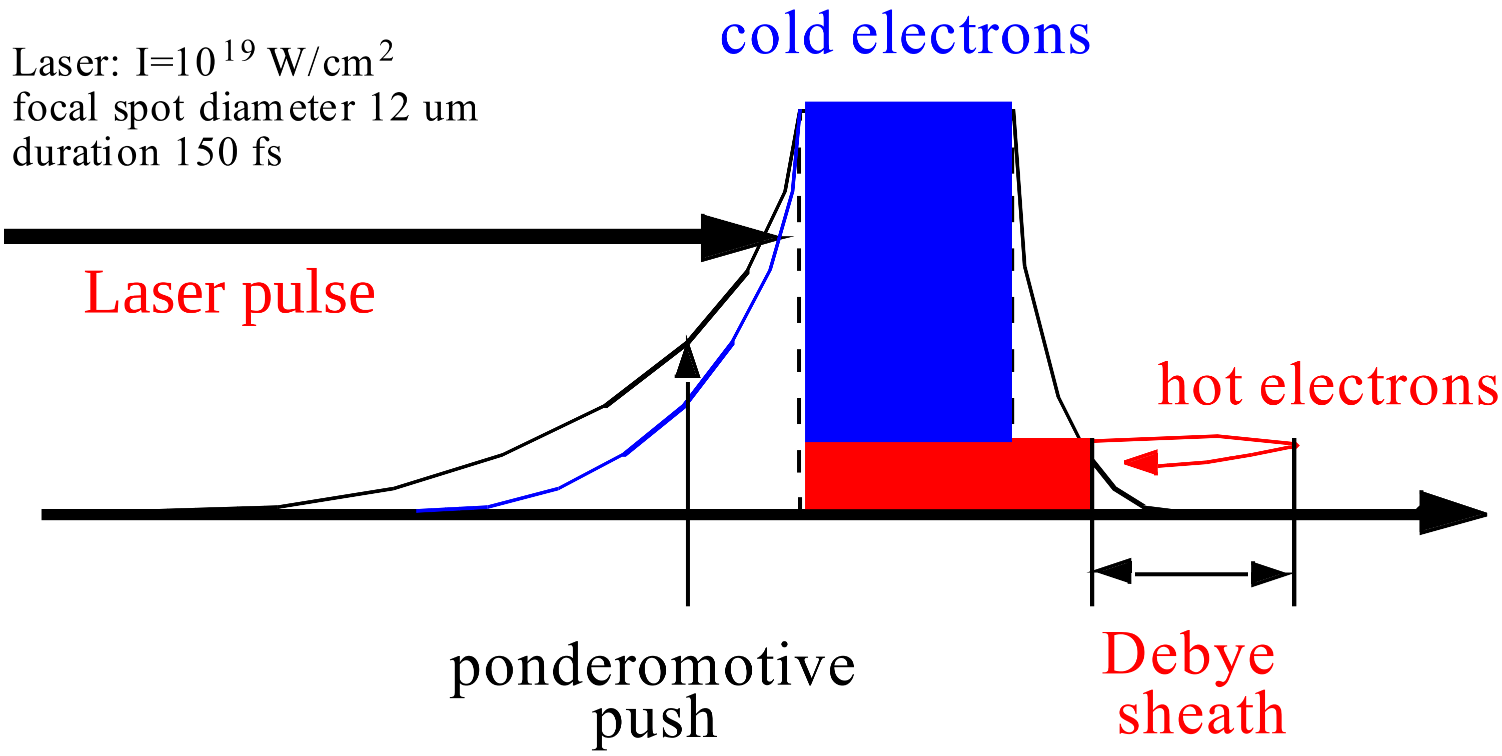

Ion acceleration from solid targets

A.Pukhov, Phys. Rev. Lett. **86**, p.3562 (2001).

Cold electrons

laser

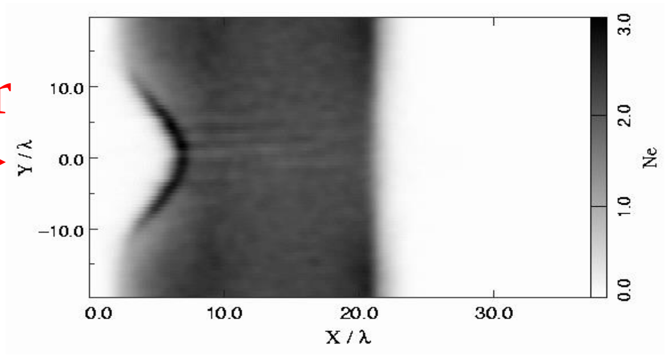

Hot electrons

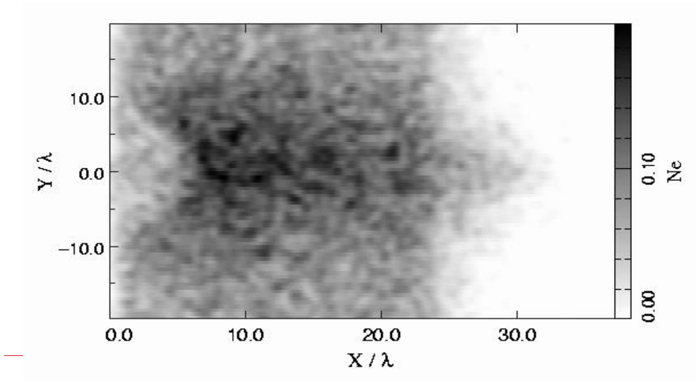

Ion energy spectrum

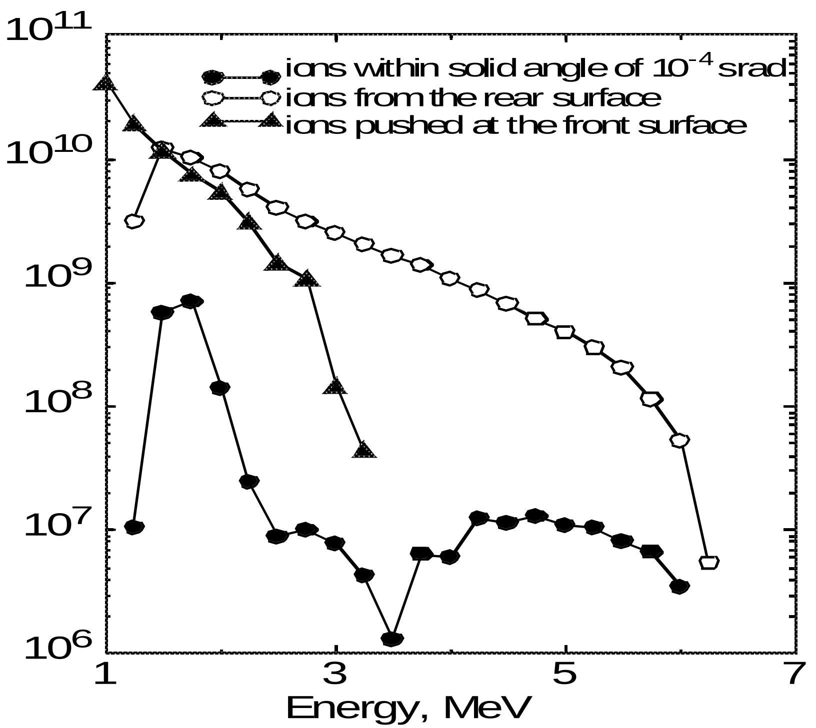

Fields in laser-solid interaction

B-field

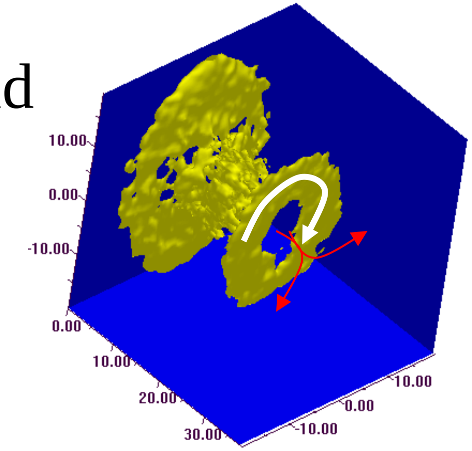

E-field

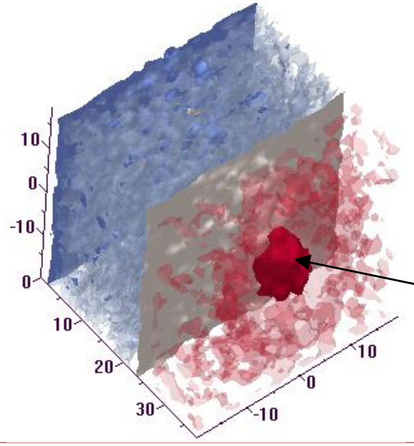

Thermal expansion

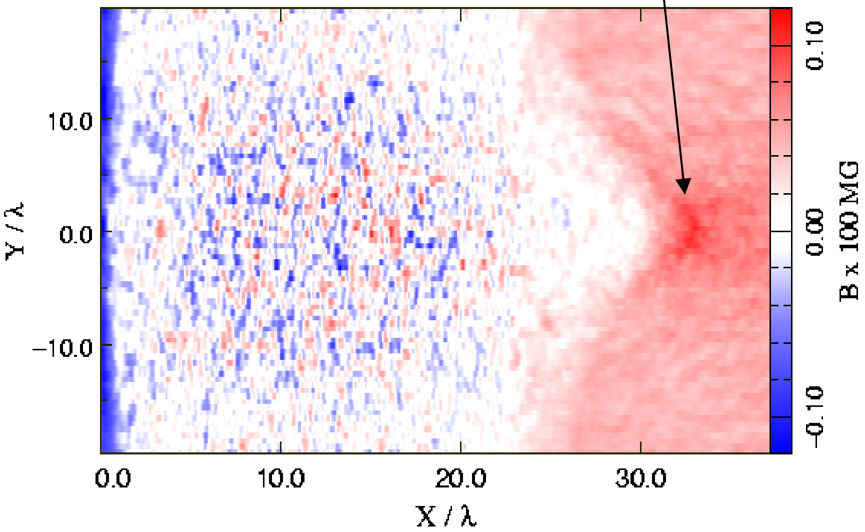

Debye sheath

Engineering interaction: Relativistic plasma nanophotonics

HEINRICH HEINE UNIVERSITÄT DÜSSELDORF

Why structured plasmas?

1. **Laser technology allows for clean relativistic pulses**
2. **Nanotechnology and 3D printing provide quite involved regular target structures at nano- and micro-scales**

What we expect?

1. **Higher absorption efficiencies at higher densities**
2. **New non-linear physics**

Relativistic plasma nano-photonics

Purvis et al. *Nature Photonics* (2013)

"**Nanograss**":
array of nanowires.

Structured material
of high average density

- What is the absorption mechanism?
- Is it a way to create **high density hot plasma**?
- What is the optimal structure?

Laser, $10^{18} \ldots 10^{20}$ W/cm^2

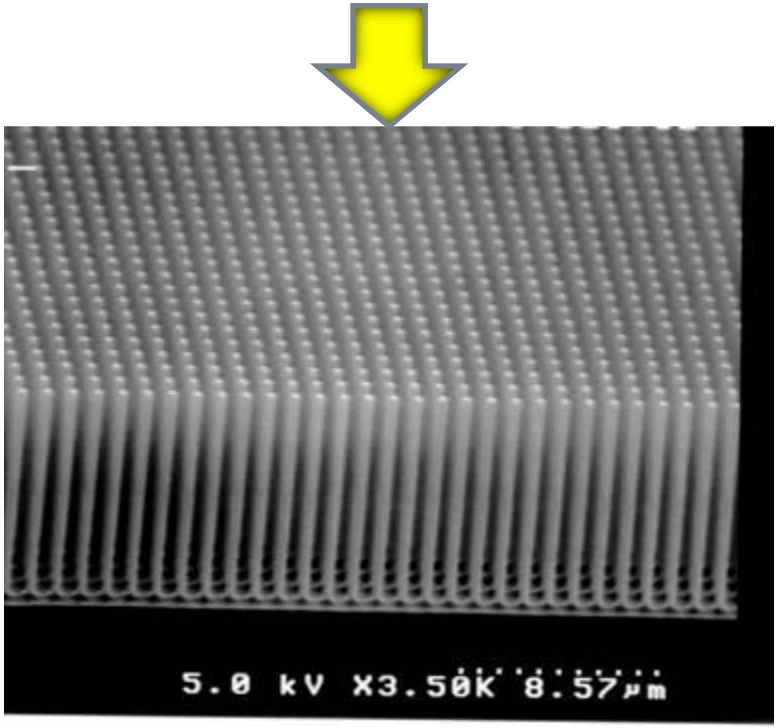

RAC Nanotech LLC

Isochoric heating of near solid density plasma

Purvis et al. *Nature Photonics* (2013)

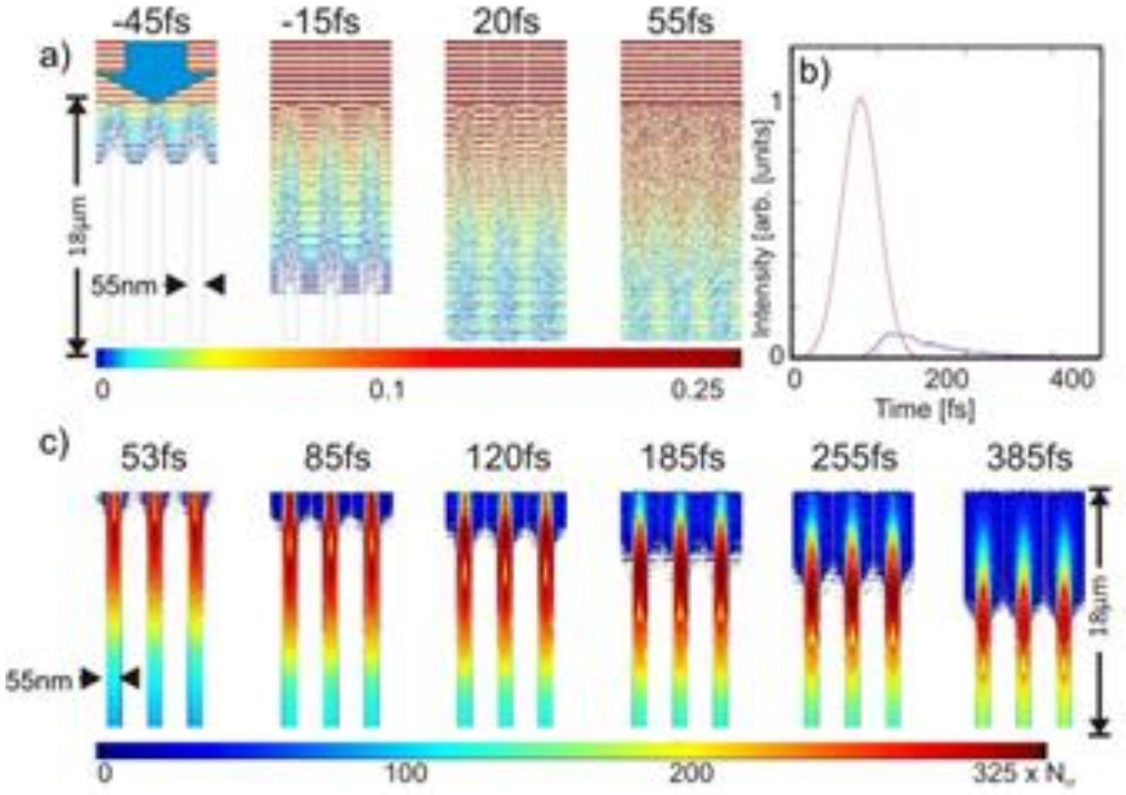

3D PIC simulation of laser beam electric field penetration in an array of vertically aligned 55 nm diameter, 18 μm long Ni wires with an average density of 12% solid density irradiated at an intensity of 5×10^{18} W/cm^2 by a λ= 400 nm, 50 fs laser pulse.

Several orders of magnitude higher x-ray yield from nanoplasmas

Purvis et al. *Nature Photonics* (2013)

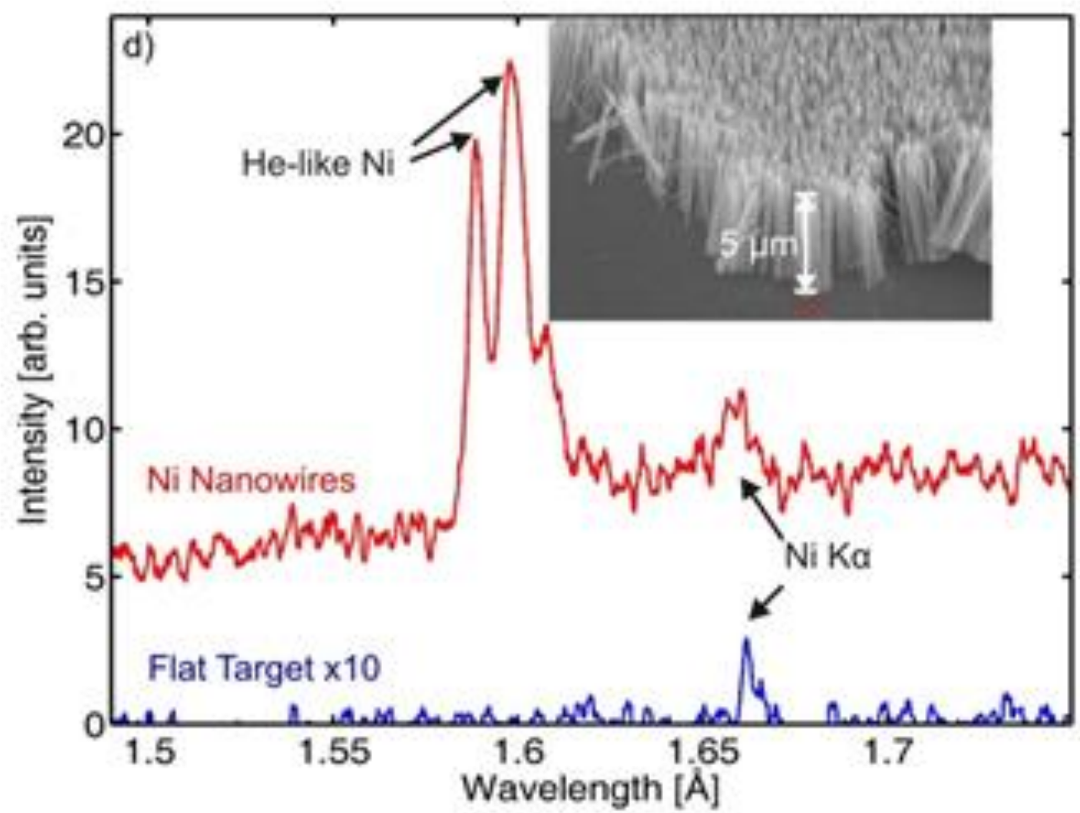

He-like Ni in 3D PIC simulations

Purvis et al. *Nature Photonics* (2013)

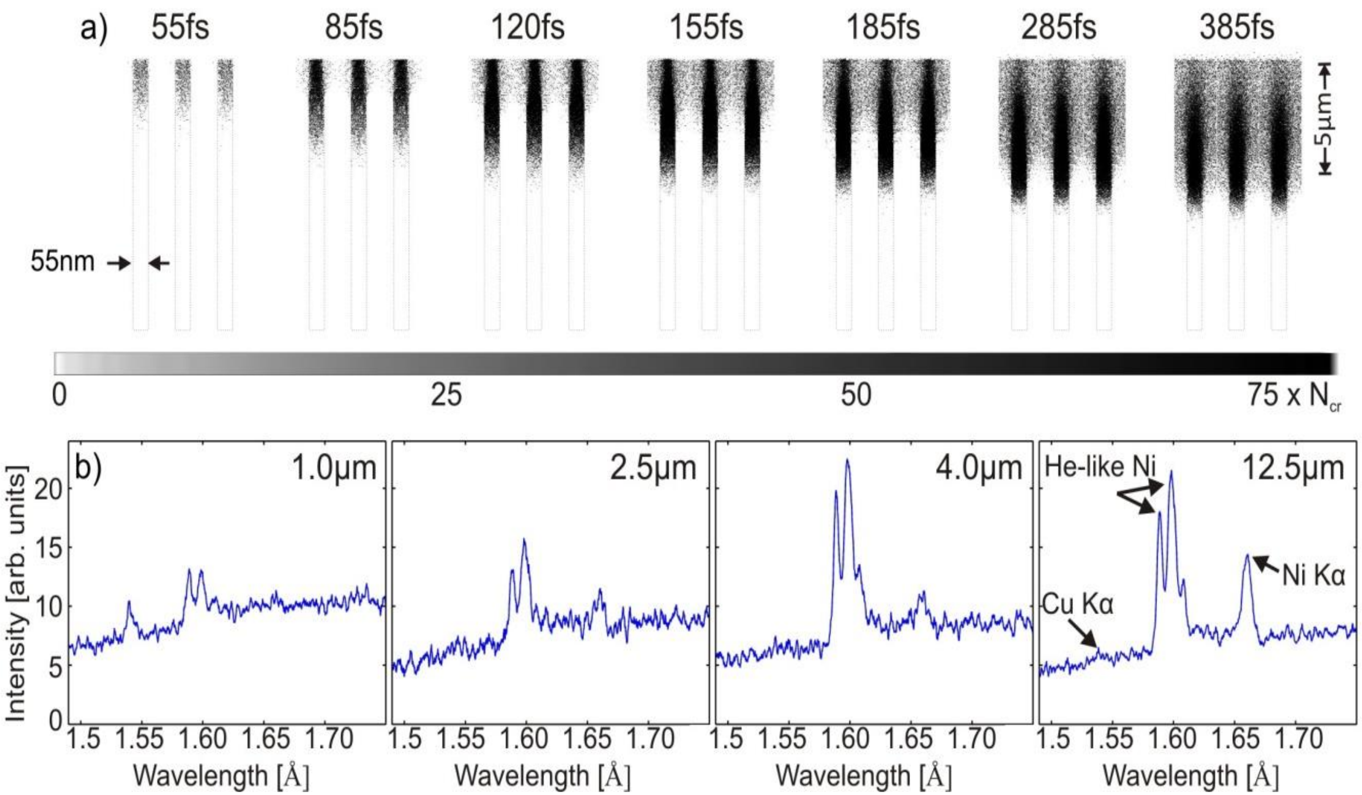

Absorption depth ~5 μm.

Radiation generation in a plasma micro-channel

Longqing Yi *et al.* PRL (2016), accepted

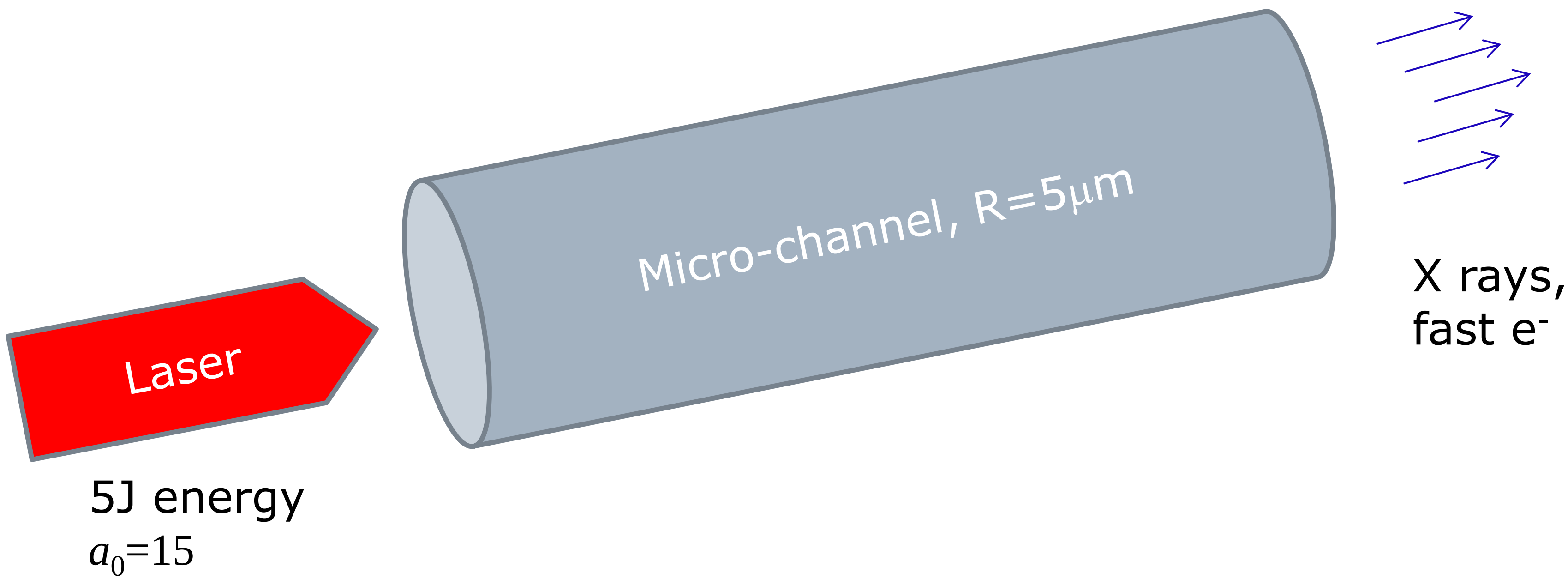

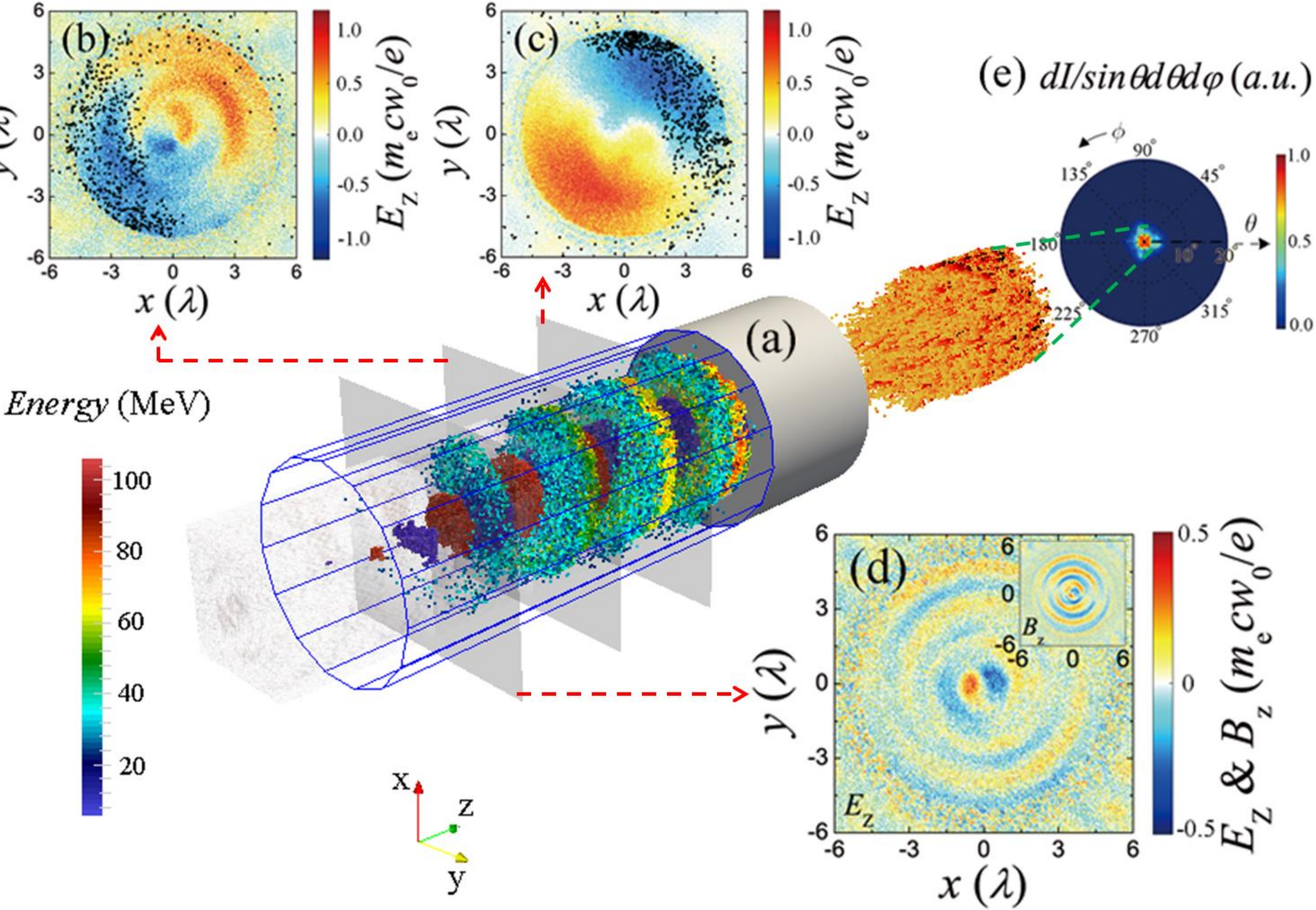

(a)
(b)
(c)
(d)
(e) dI/sinθdθdφ (a.u.)
Energy (MeV)
x (λ)
y (λ)
E_z (m_e cw_0/e)
E_z & B_z (m_e cw_0/e)
E_z
B_z
φ
θ
x
y
z

Radiation generation in a plasma micro-channel

Longqing Yi *et al.* PRL (2016), accepted

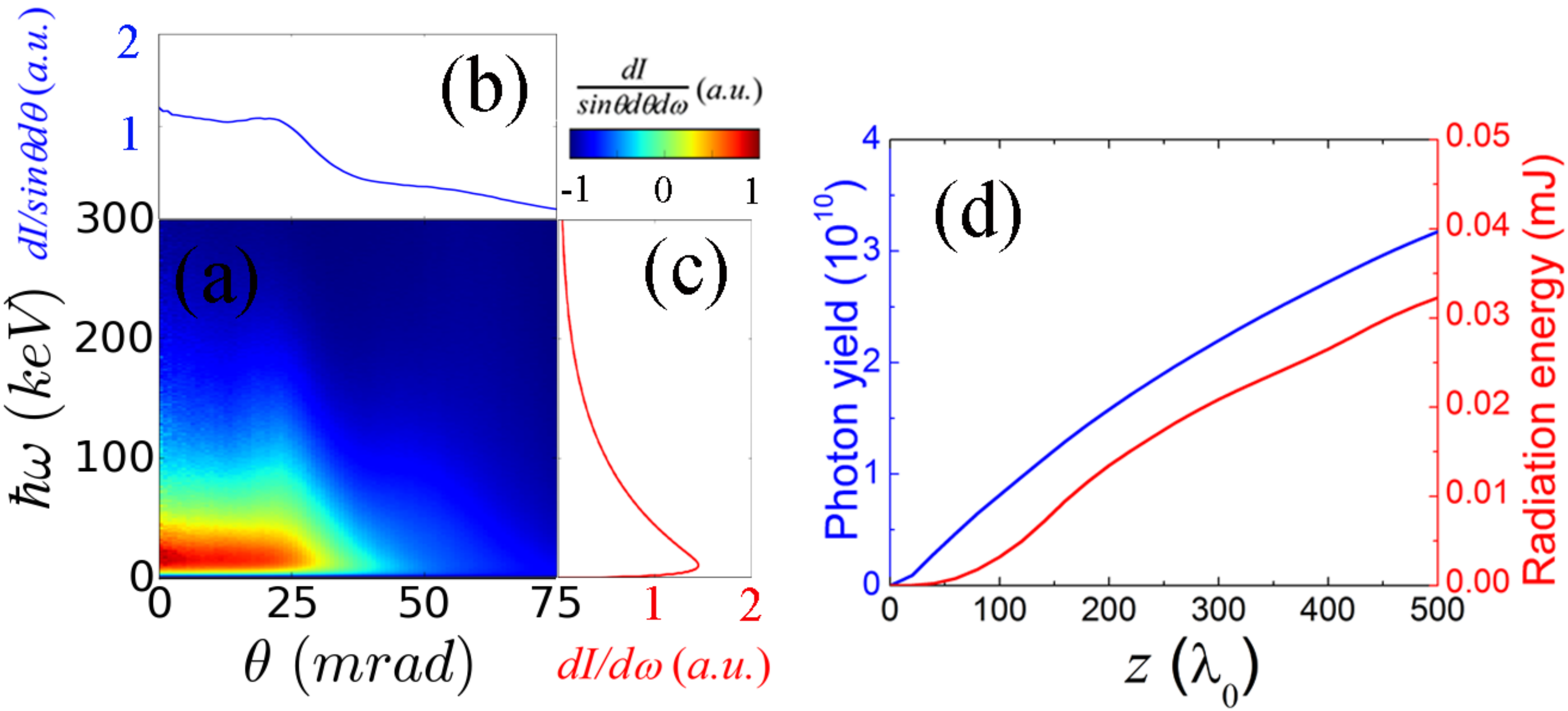

Radiation generation in a plasma micro-channel

Longqing Yi *et al.* PRL (2016), accepted

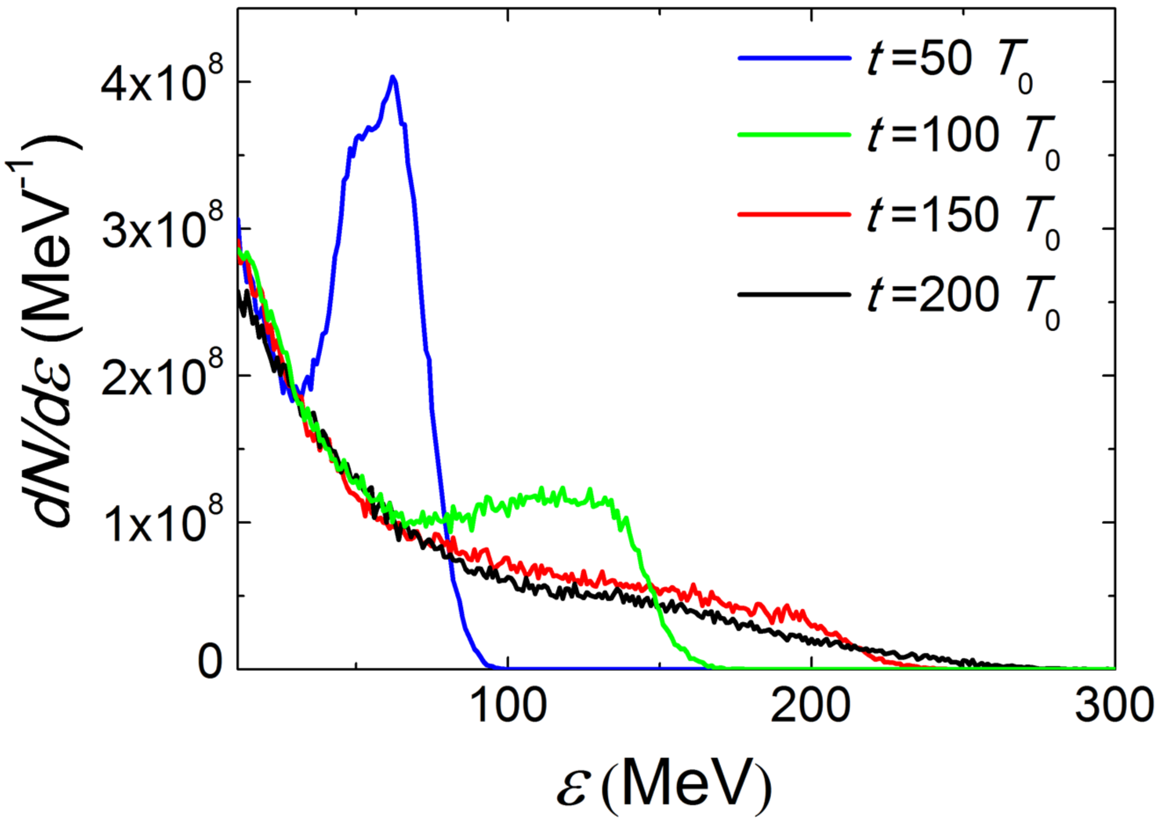

Radiation generation in a plasma micro-channel

Longqing Yi *et al.* PRL (2016), accepted

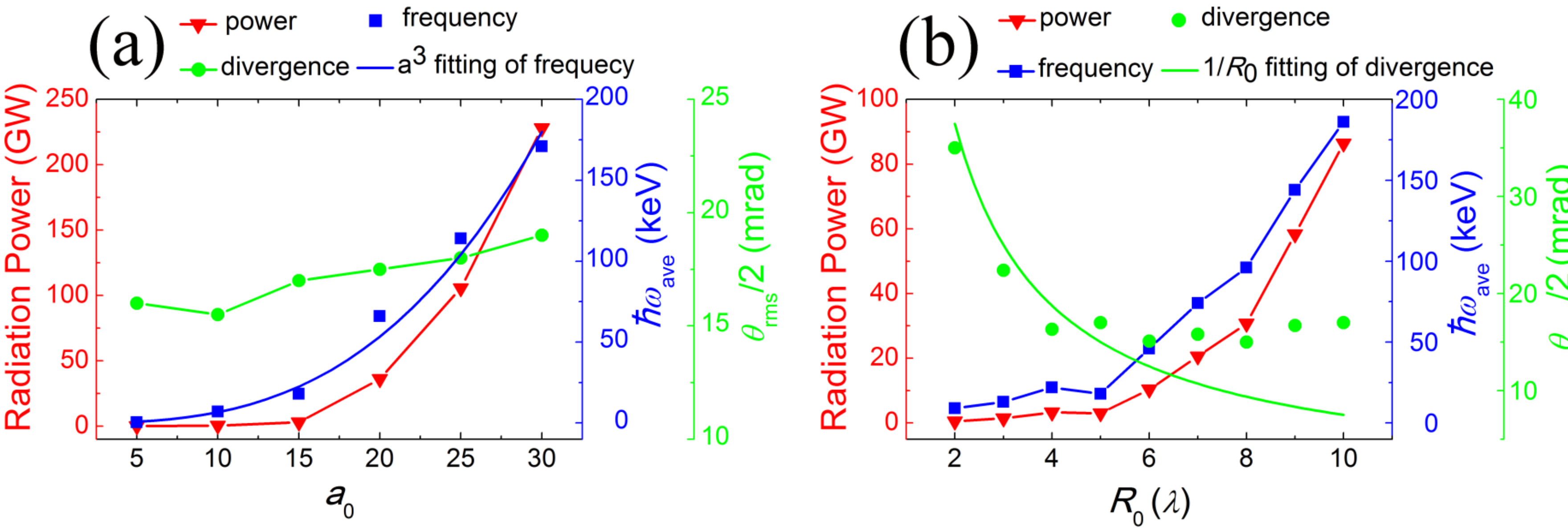

Radiation generation in a plasma micro-channel

Longqing Yi *et al.* PRL (2016), accepted

Bright photon source

1.2×10^{10} photons at 20 keV in $\Delta\theta$=50 mrad

Peak spectral intensity of

1.8×10^{17} photons/mrad /s/0.1% bandwidth.

Relativistic microoptics

Jiang et al., *PRL* (2016)

Microwire array:
Laser guiding, focusing
enhanced electron
heating

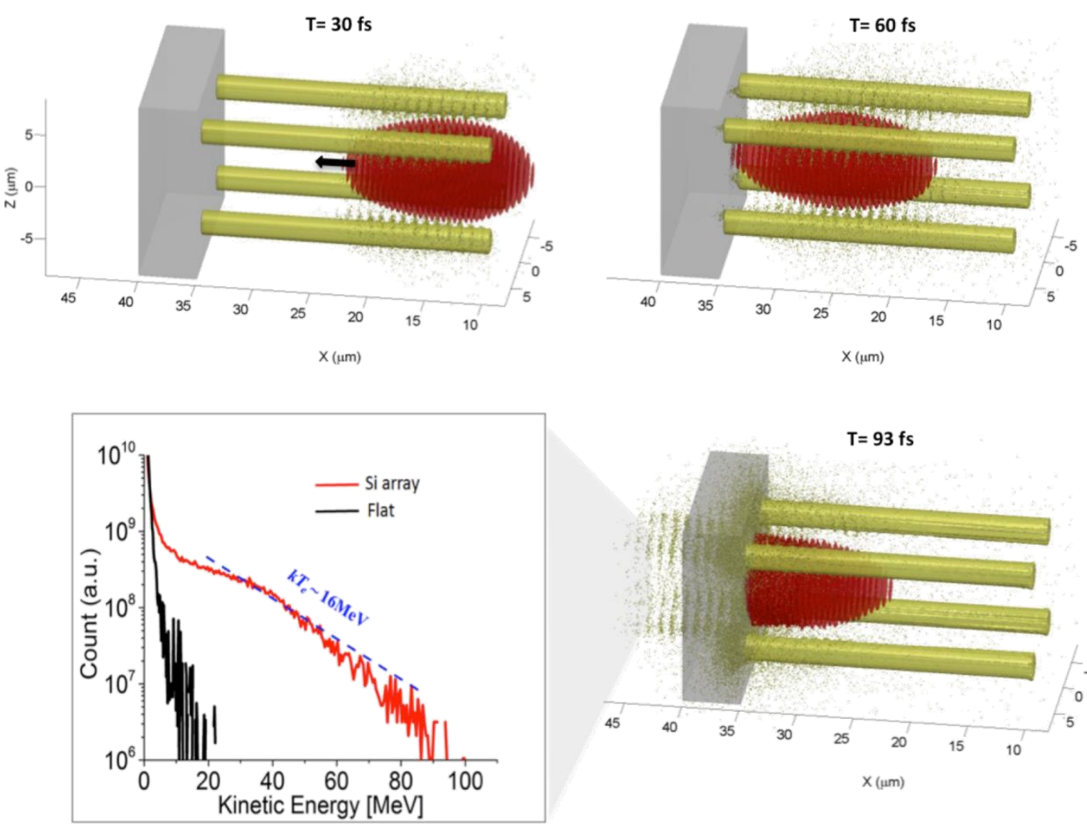

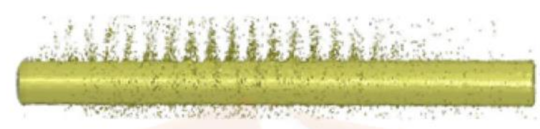

Relativistic microoptics global focusing of the laser

Jiang et al., *PRL* (2016)

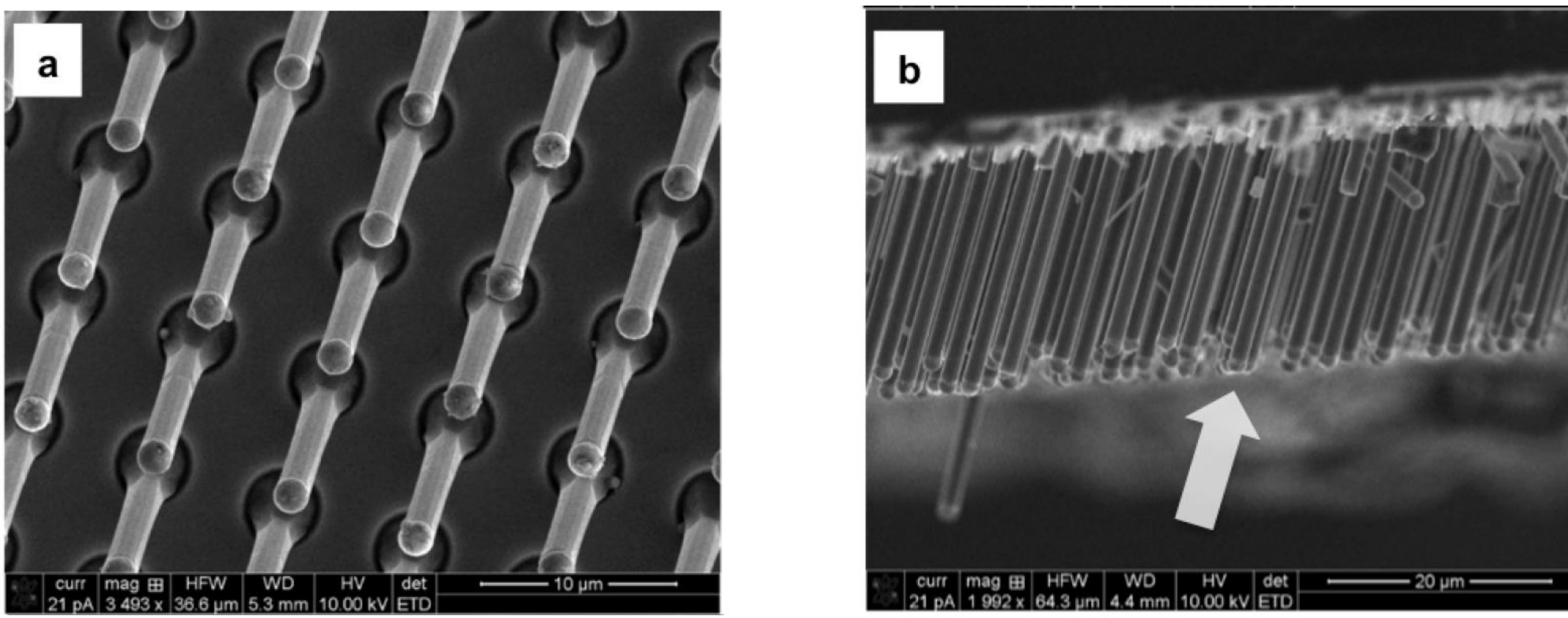

A scanning electron microscope (SEM) images of microphotonics targets:
a, top view showing wire spatial distribution.
b, side view showing the orientation of the wires

Relativistic microoptics

Jiang et al., *PRL* (2016)

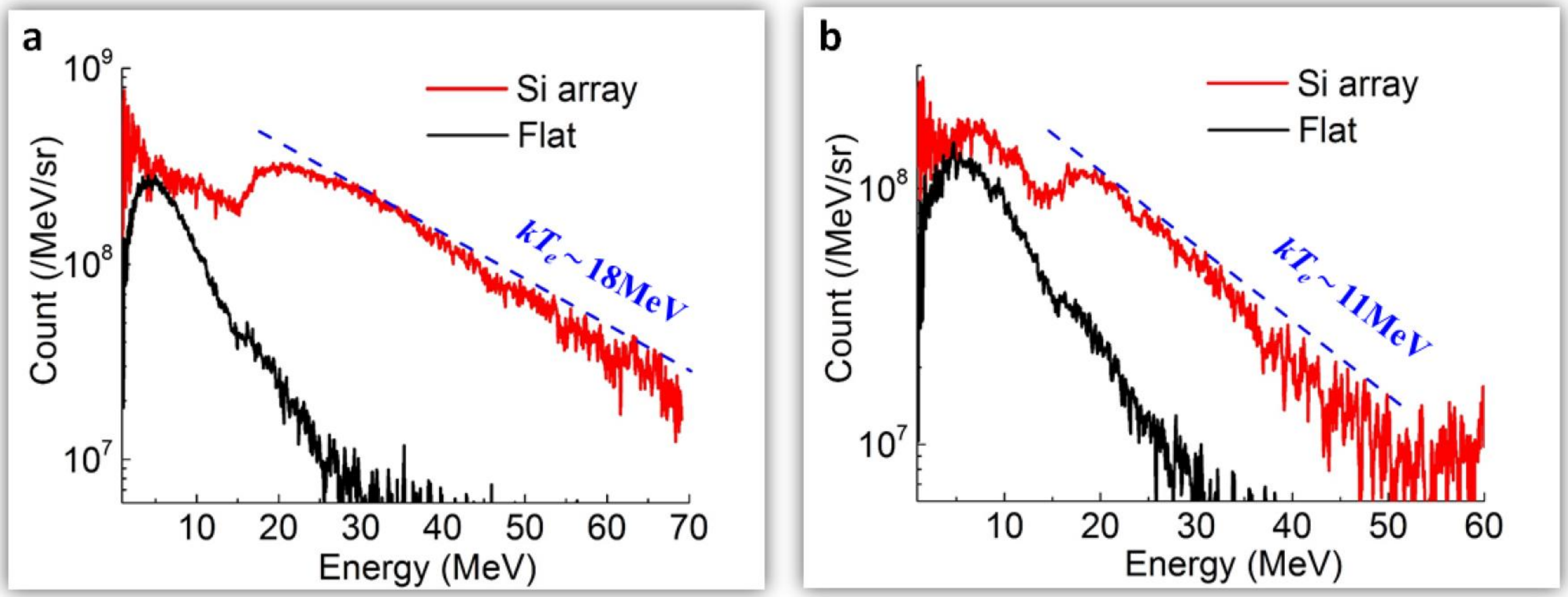

Experimental results: electrons spectra for 4 laser shots.
Flat target spectra (blue), Si arrays spectra (green).

HEINRICH HEINE
UNIVERSITÄT DÜSSELDORF

Relativistic microoptics

Jiang et al., *PRL* (2016)

Averaged field structure around the microwire

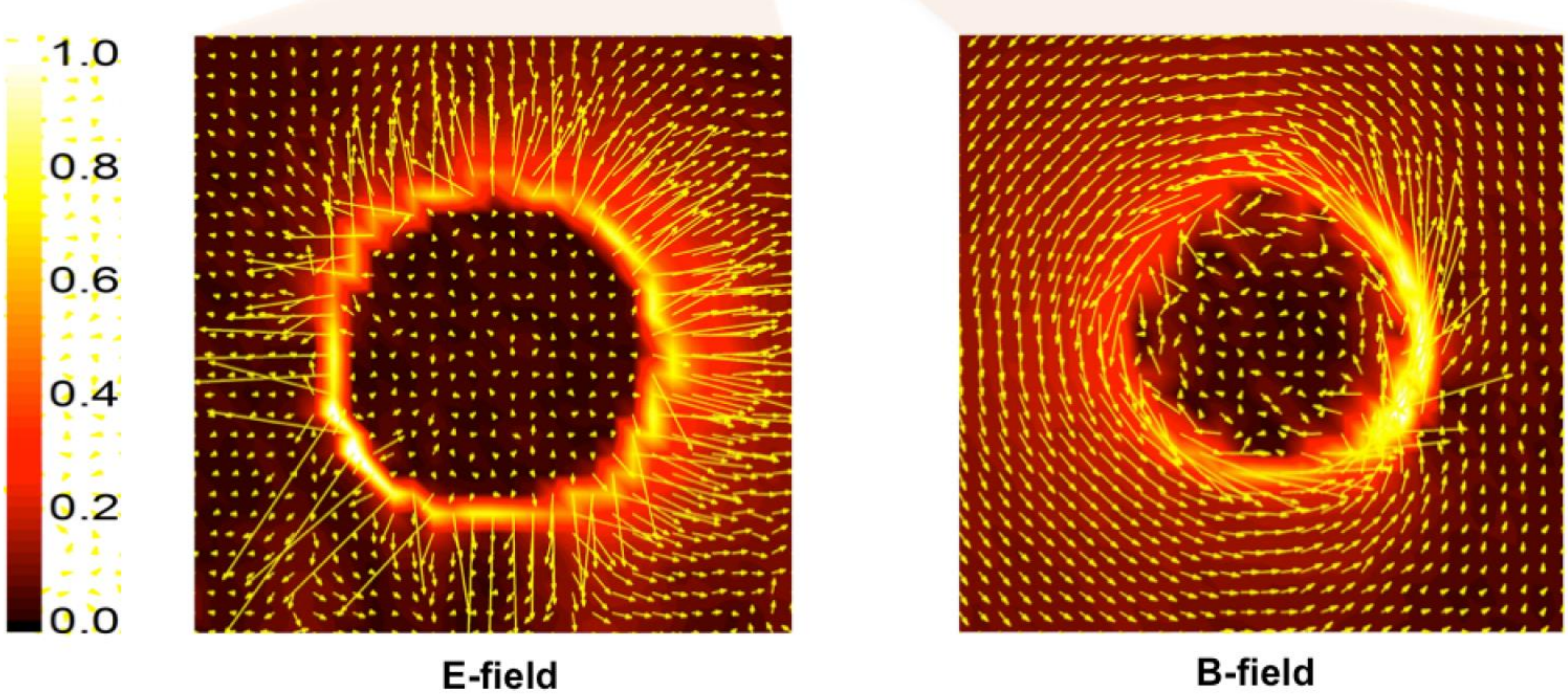

Microcone interaction

D. Zhou et al. *Phys. Plasmas* (2015)

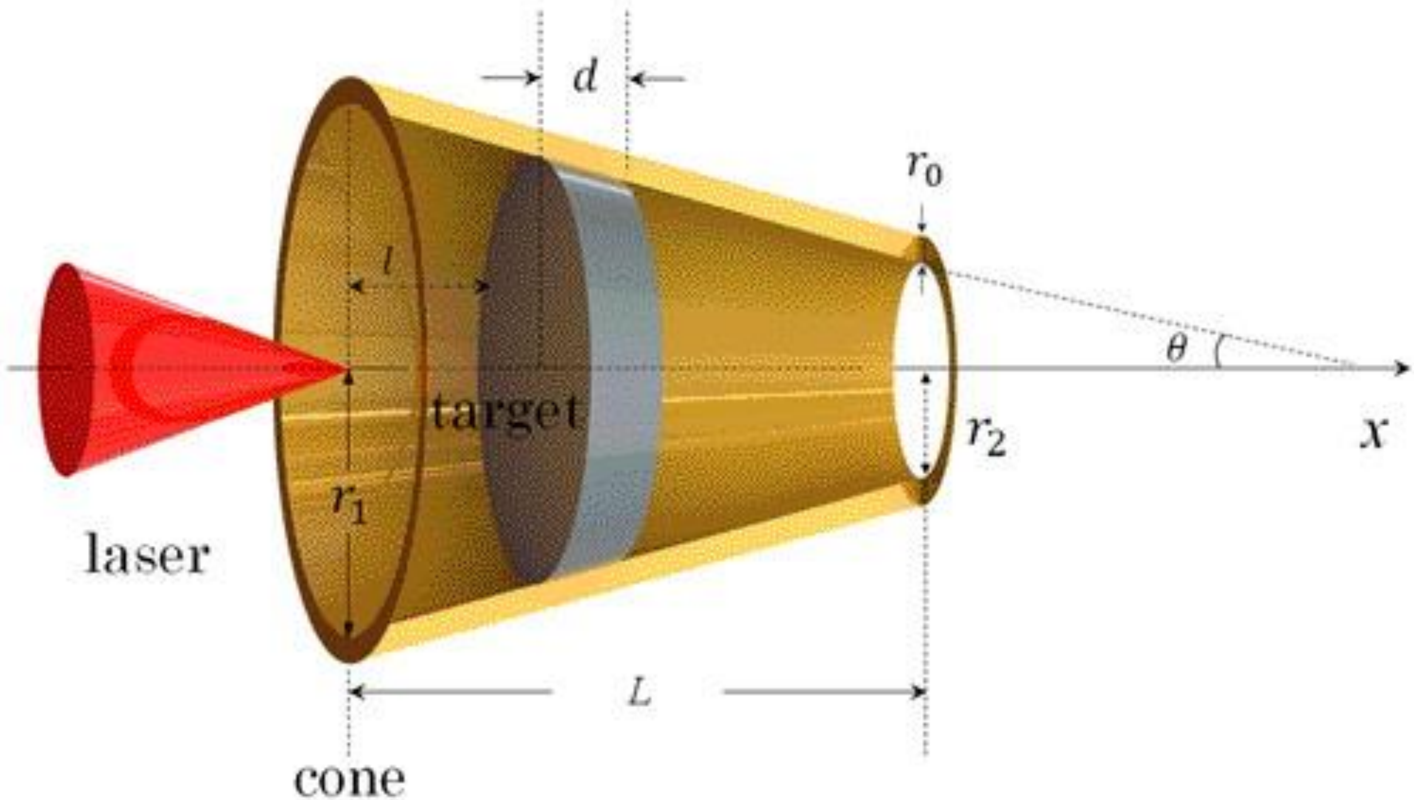

Microcone interaction

D. Zhou et al. *Phys. Plasmas* (2015)

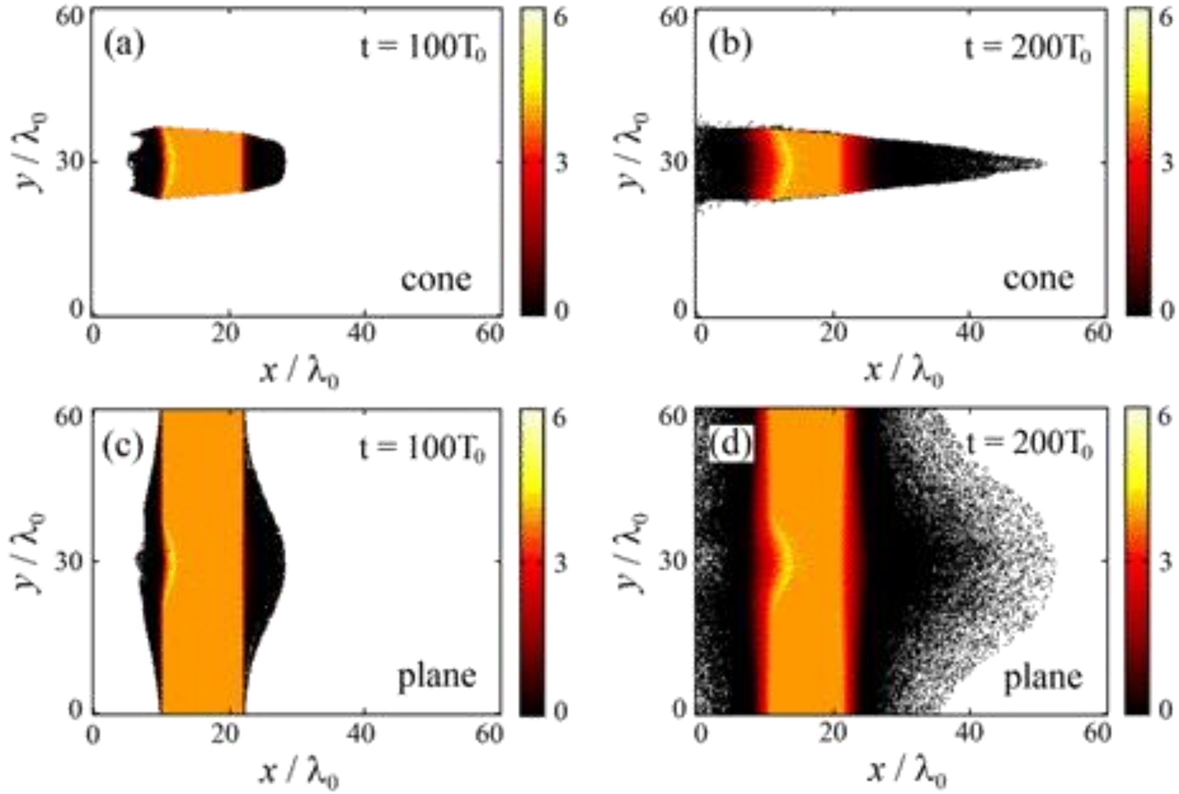

Protons for both cone and plane targets cases at t = 100 and 200. Here, the density is normalized by the critical density

Microcone interaction

D. Zhou et al. *Phys. Plasmas* (2015)

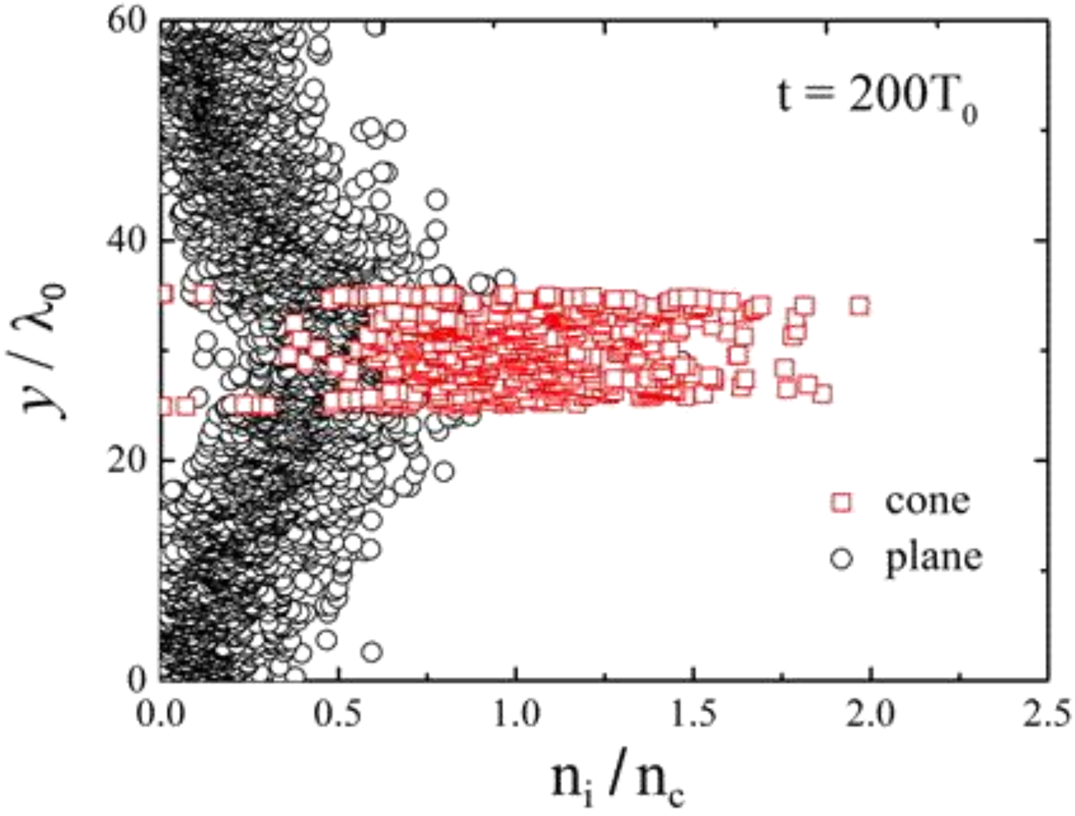

The average proton density at t = 200 for the cone (red squares) and plane (black circles) target cases.

Microcone interaction

D. Zhou et al. *Phys. Plasmas* (2015)

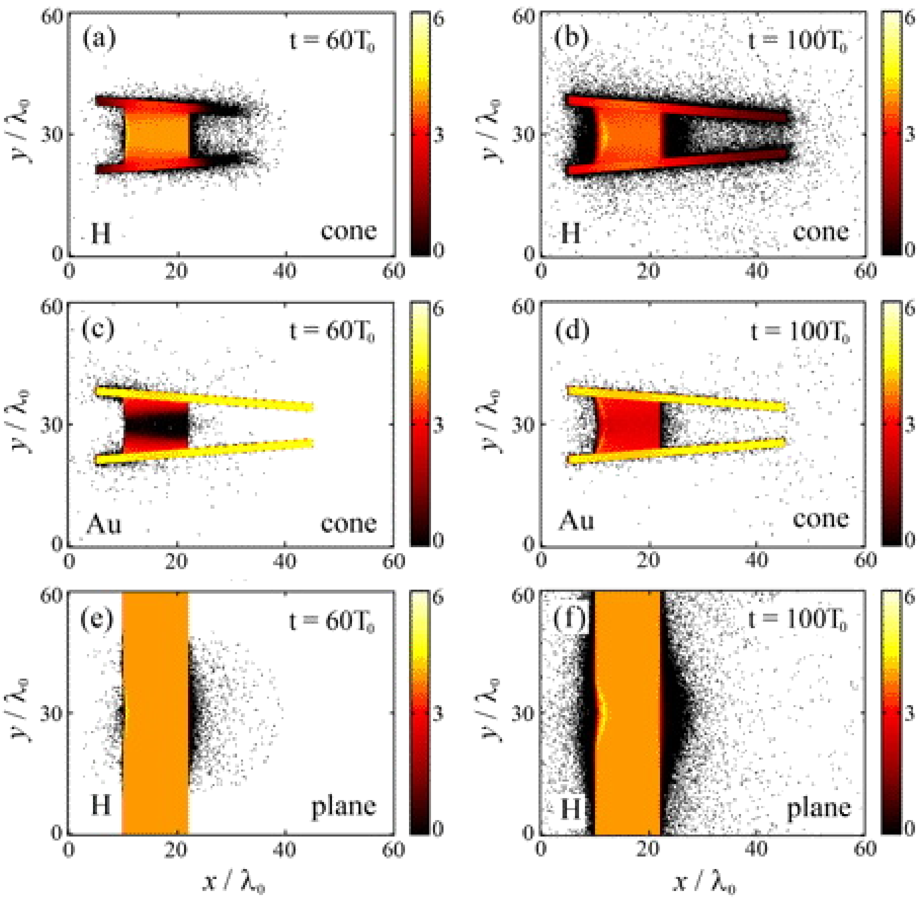

The electron density distribution of the solid target [(a) and (b)] and the guiding cone [(c) and (d)] for cone target case at t = 60 and t = 100.

For comparison, the electron density distribution for the plane target case is presented in (e) and (f).

Microcone interaction

D. Zhou et al. *Phys. Plasmas* (2015)

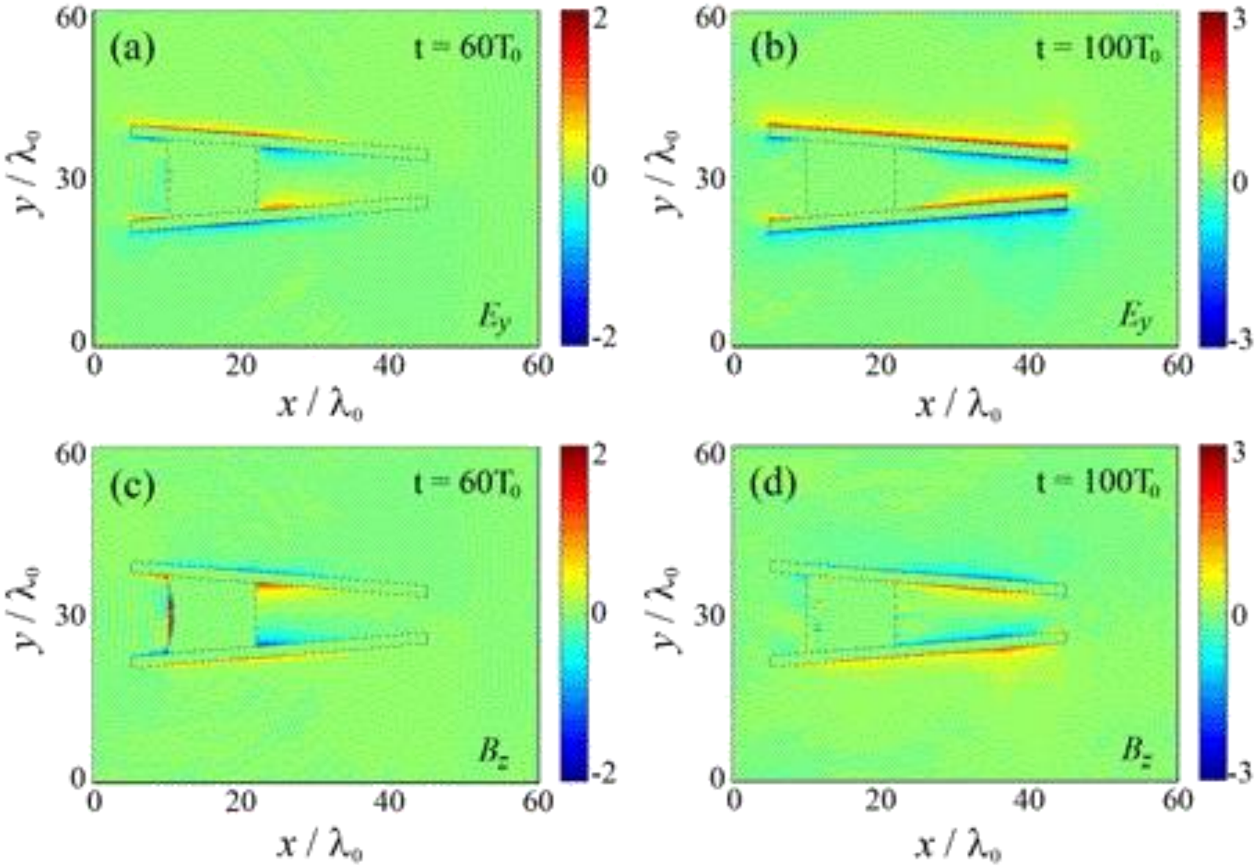

Quasi-static fields
Ey [(a) and (b)]
Bz [(c) and (d)]
for the cone target

Microcone interaction

D. Zhou et al. *Phys. Plasmas* (2015)

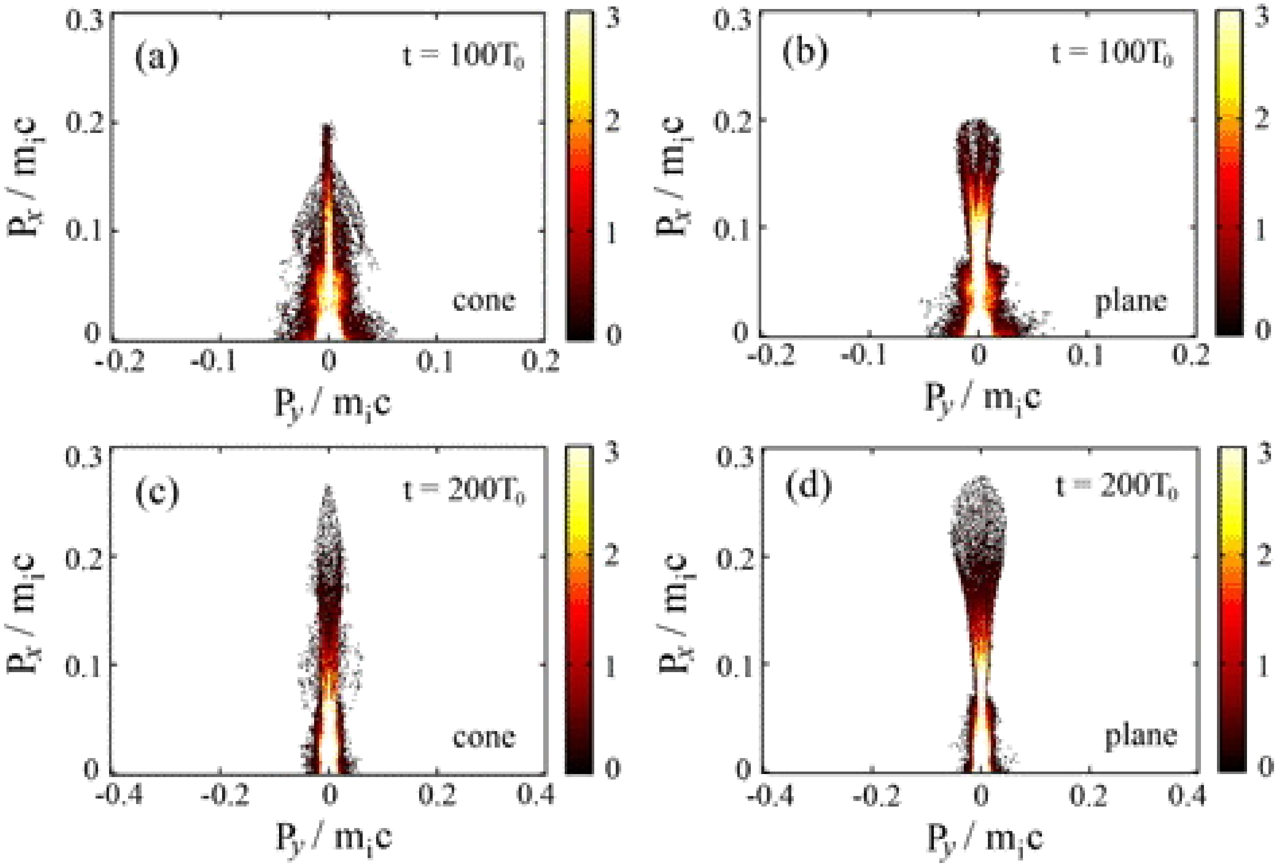

Proton momentum for the cases of cone [(a) and (c)] plane [(b) and (d)] at t = 100 and t = 200

Microcone interaction

D. Zhou et al. *Phys. Plasmas* (2015)

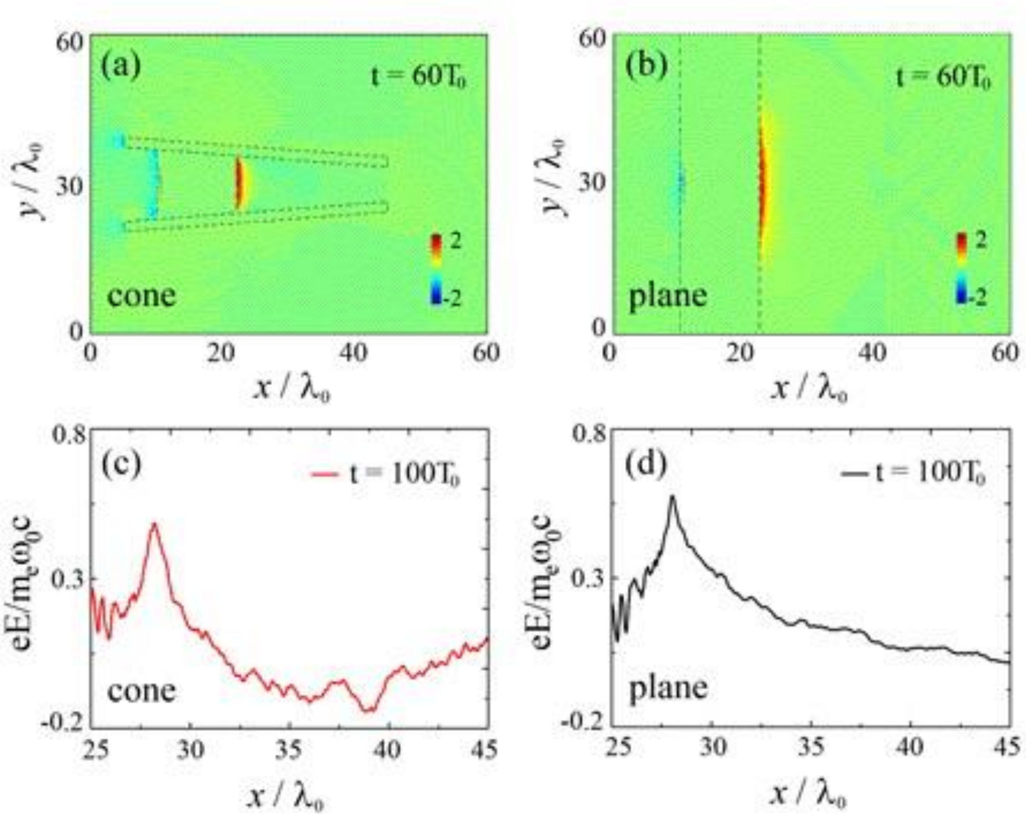

Longitudinal field Ex
and the axial profiles
along the laser axis
for the cone [(a) and (c)]
and plane [(b) and (d)]
at t = 60 and t = 100

Microcone interaction

D. Zhou et al. *Phys. Plasmas* (2015)

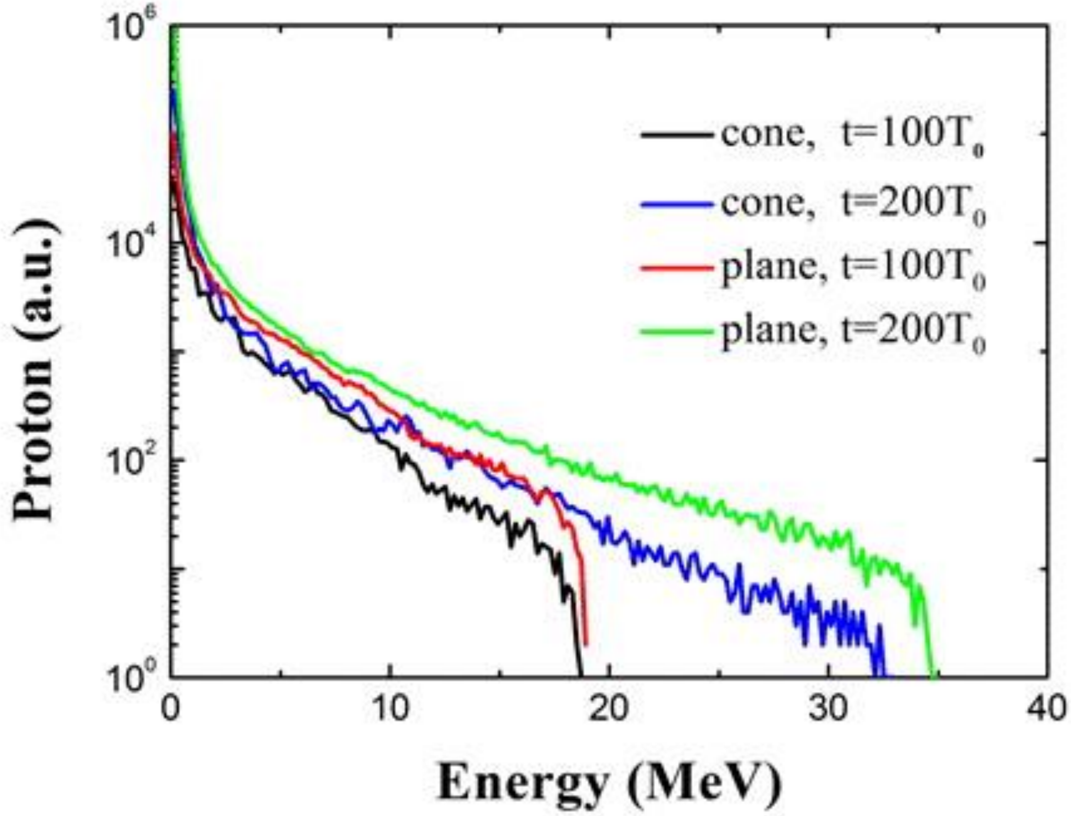

Proton energy spectra

Ion acceleration: Sailing on the light

Ion acceleration from nanofoils
Light Sail Regime

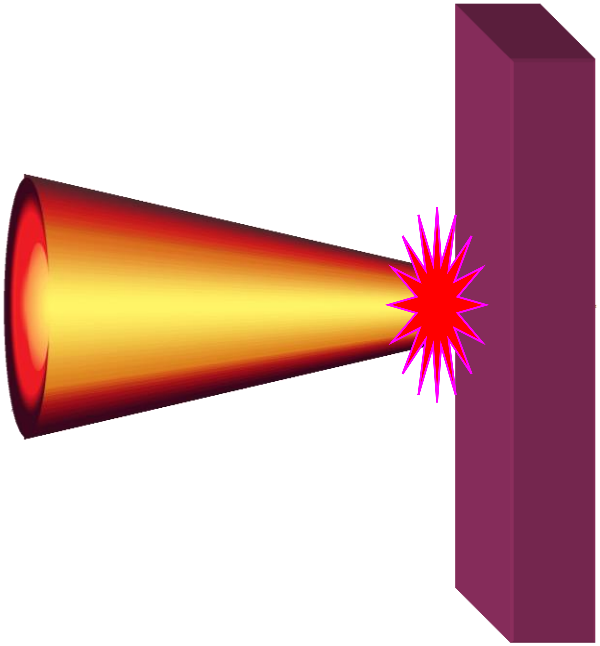

Light pressure:

$$P = \frac{I}{c} \approx 3.3\ \text{GBar} \ \ \text{for} \ \ I = 10^{19}\ \text{W/cm}^2.$$

Thin nanofoils can be accelerated to relativistic velocities by the laser pressure in the "Light Sail Regime"

Thin foils: light sail regime circularly polarized laser pulse

Zhang, et al., (2007), Robinson, et al., (2008); Klimo, et al., (2008); Yan, et al., (2008).

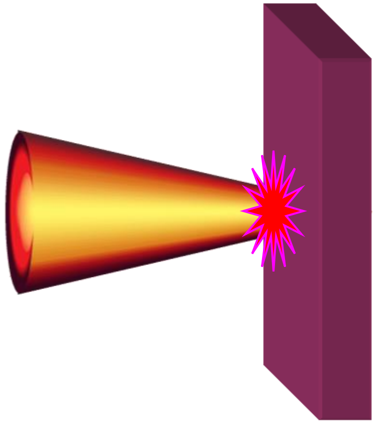

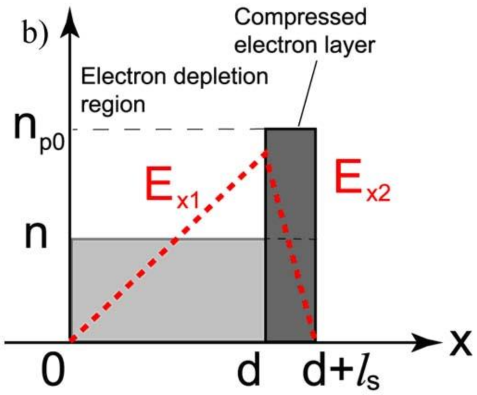

$$a_L(1+\eta)^{1/2} \sim (n_0/n_c)(D/\lambda_L).$$

To be sure the CP ponderomotive force is balanced by the charge separation field and all the ions in the target can be accelerated.

$$a_L < (n_0/n_c)(2\pi D/\lambda_L).$$

To be sure the electrons and ions are not completely separated.

3D regime of light sail: Gaussian pulse

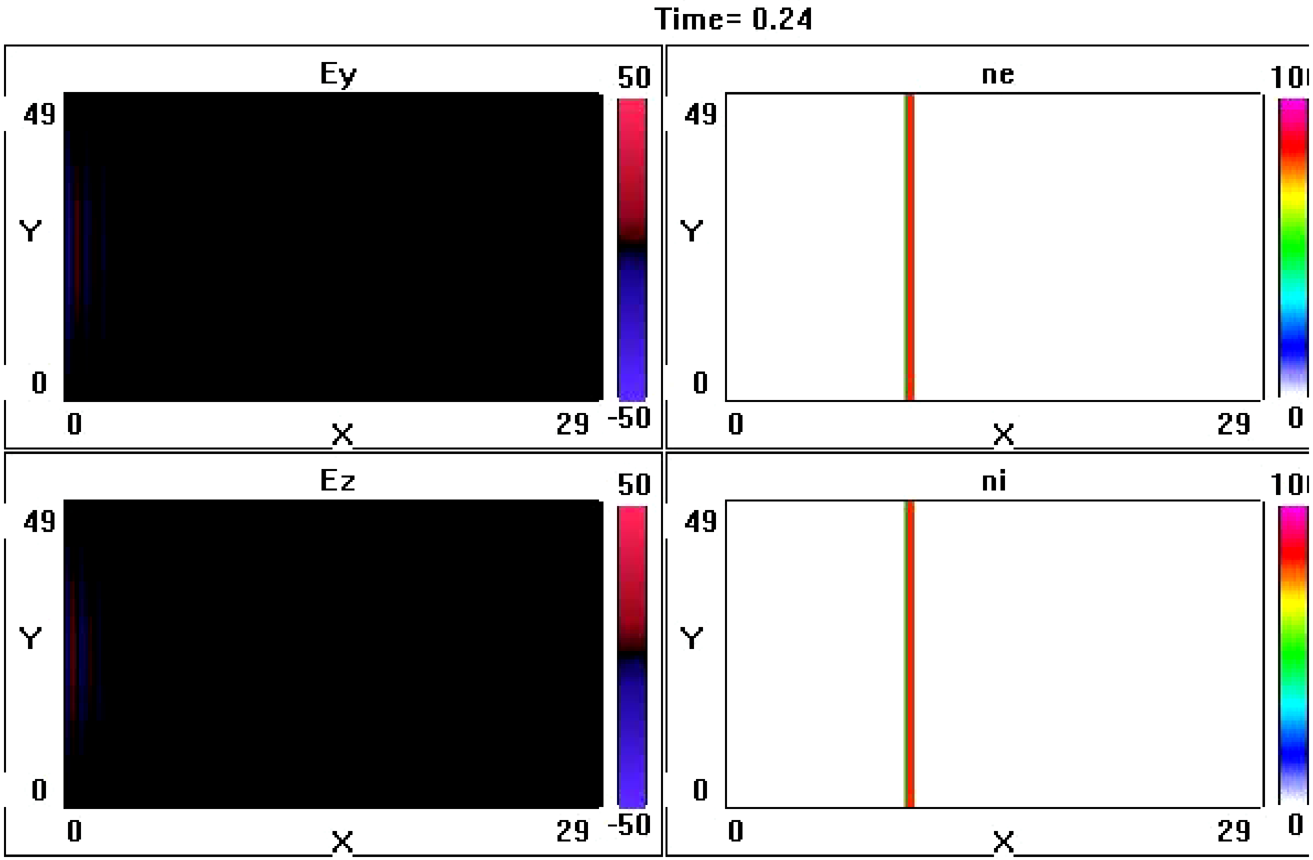

a=50

τ=26 T_L

σ_r=5λ

n/n_c=80

L=0.5λ,

M. Chen, T.P.Yu, A. Pukhov, Z.M.Sheng PRL 2009

Shaped foil target (SFT)

In the regime of RPA, the foil motion equation:

$$\frac{d\beta}{dt} = \frac{E_L^{\ 2}}{2\pi\rho c}(1-\beta)^2\sqrt{1-\beta^2}, \ p = mnlv = \rho v, \rho = mnL$$

Foil area mass density

For Gaussian Laser pulse:

$$E_L^{\ 2} \propto \rho \propto nmL$$

$$E_L = E_0 \, e^{(-r^2/\sigma_L^{\ 2})}$$

$$L = L_0 \, e^{(-r^2/\sigma_T^{\ 2})}$$

$$\sigma_L \approx \sqrt{2}\sigma_T$$

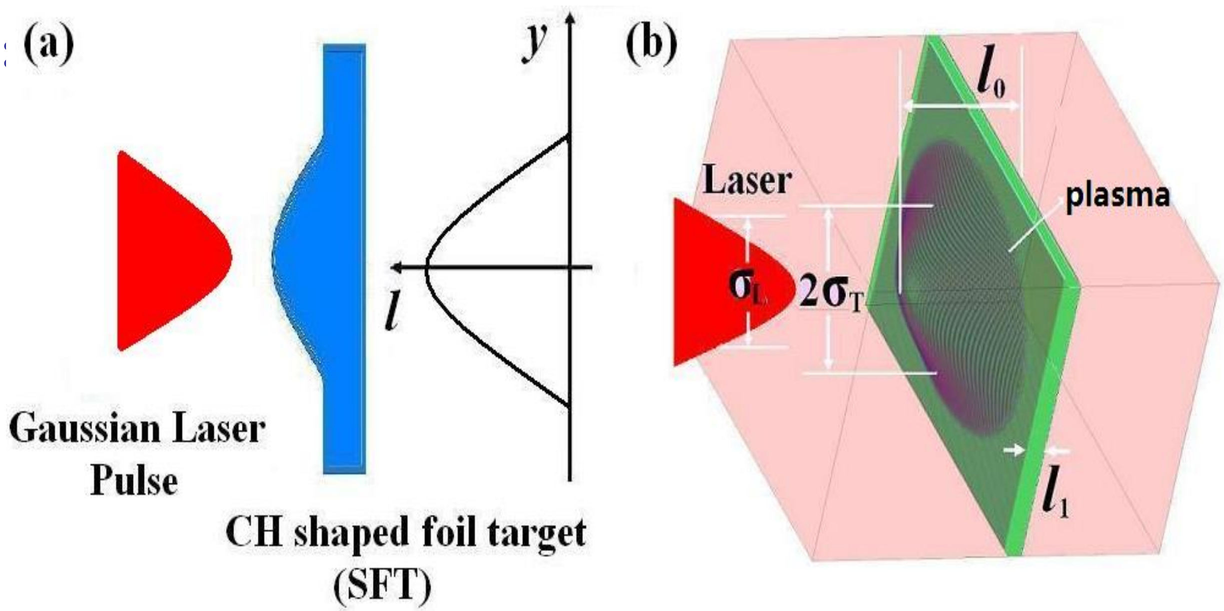

See references here:

M. Chen et al., PRL 103, 024801 (2009)

T.P. Yu et al., Laser Part. Beams 27, 611 (2009)

M. Chen et al., New J. Phys. 12, 045004 (2010)

3D Simulation Results

VLPL

Shaped target

Chen, Yu, Pukhov, Sheng *PRL* (2009)

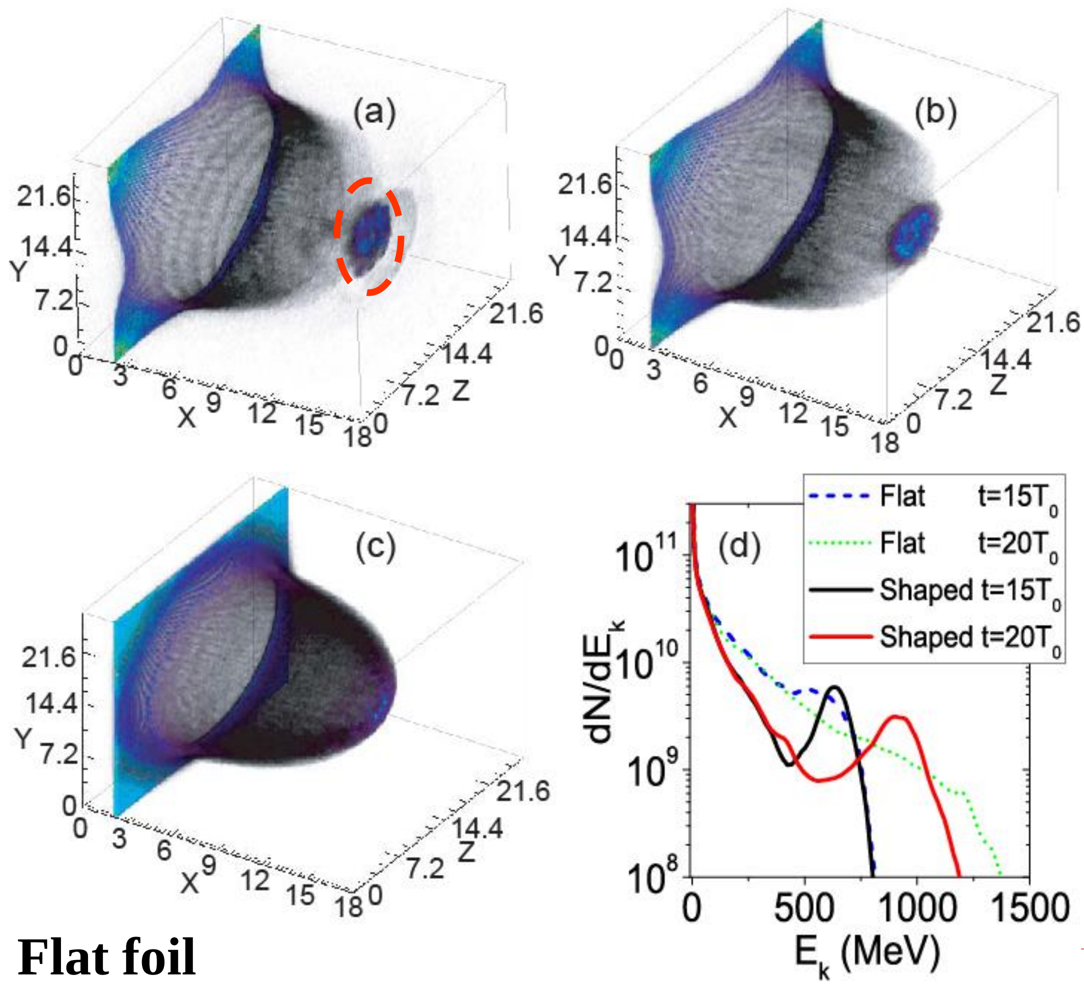

Flat foil

$t=20T_0$
3D simulation:
N_e and N_i

Well-defined proton bunch for the shaped foil target

Two-specie targets. CH foil

HEINRICH HEINE
UNIVERSITÄT DÜSSELDORF

Yu, Pukhov, Shvets, et al. *PRL* **105**, 065002 (2010)

Protons are quickly separated from carbons
Protons build up a dense layer on top of heated carbon cloud

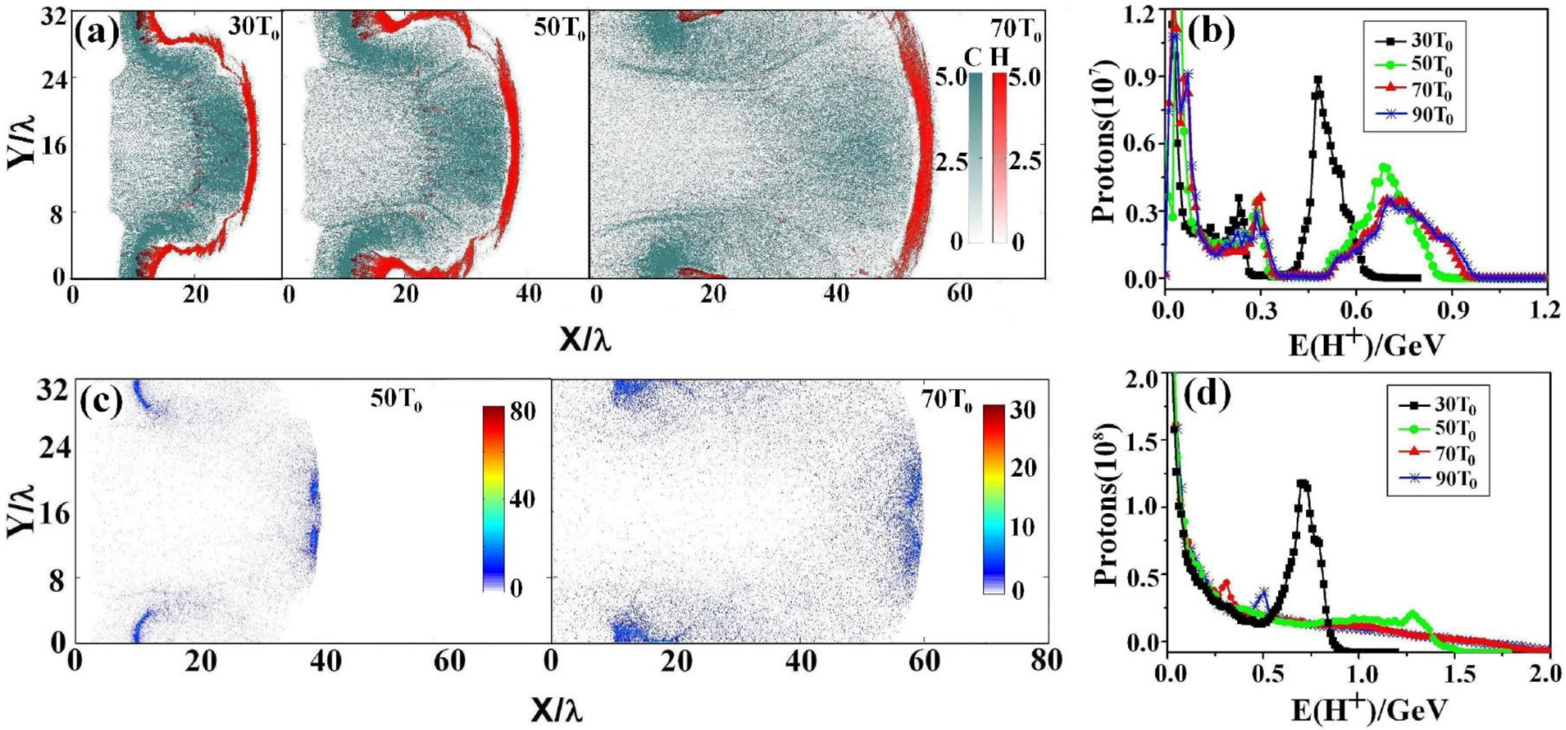

CH foil

Pure
H target

Limit of light sail acceleration: GeV/u

$$\rho \frac{d(\gamma\beta)}{dt} = \frac{E_l^2}{2\pi c}\frac{1-\beta}{1+\beta} \qquad \rho = \sum_i m_i n_i l \text{ – foil area mass density}$$

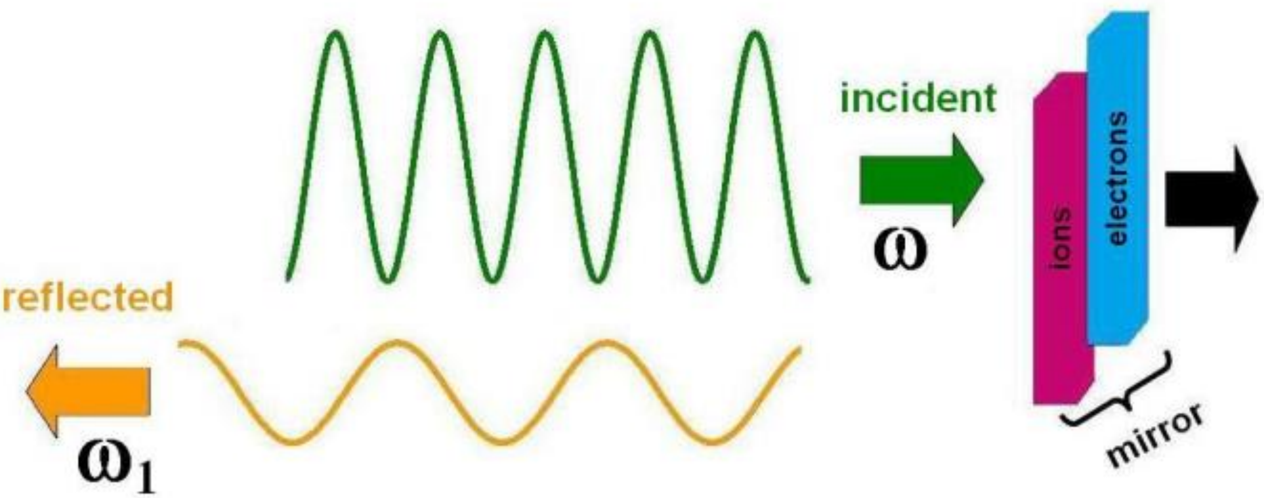

$$\frac{\omega_1}{\omega} = \frac{1-\beta}{1+\beta} \approx \frac{1}{4\gamma^2}$$

$$\eta = 1 - \frac{1}{4\gamma^2}$$

$$\gamma = \frac{1}{\sqrt{1-\beta^2}}$$

Limit of light sail acceleration: GeV/u

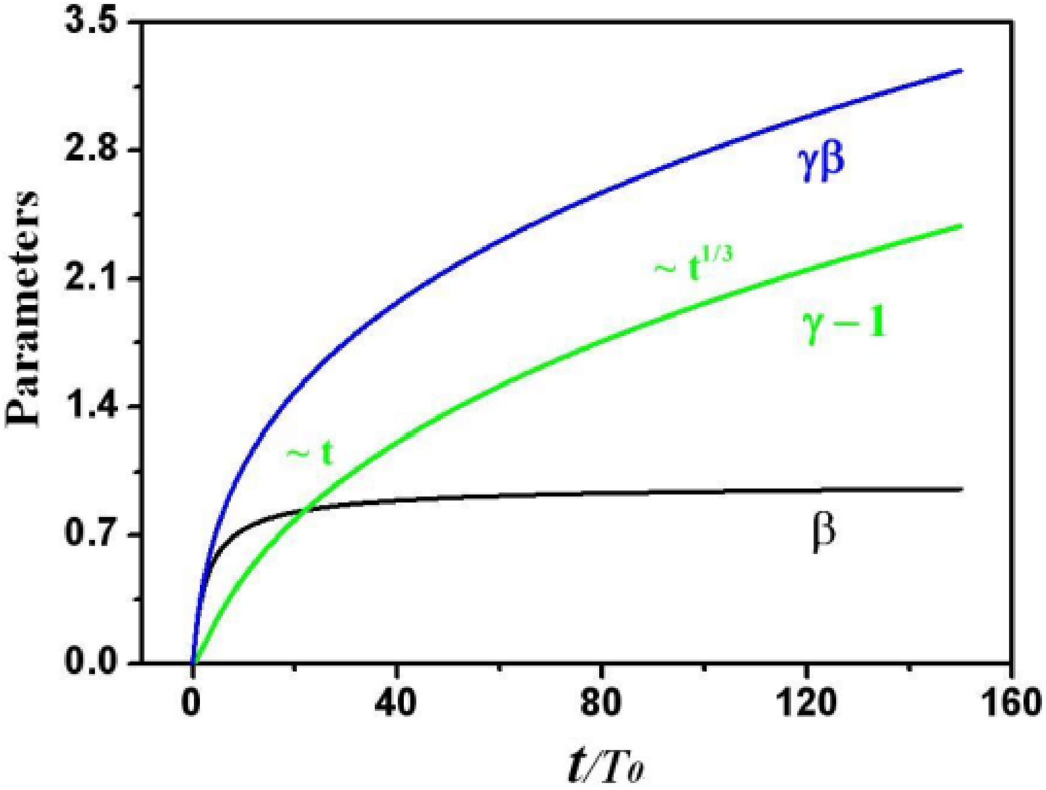

$$\rho \frac{d(\gamma\beta)}{dt} = \frac{E_l^2}{2\pi c}\frac{1-\beta}{1+\beta}$$

$$p + \frac{2}{3}\left(p^3 + \gamma^3\right) = 2a^2\omega t + \frac{2}{3}$$

Required laser power scales as γ^3 when $\gamma >> 1$

Light Sail Acceleration does not work for highly relativistic ions

Light Sail Drag Field Acceleration

Ji, Pukhov, Shen, *New Journal of Physics* ***16****, 063047* (2014)

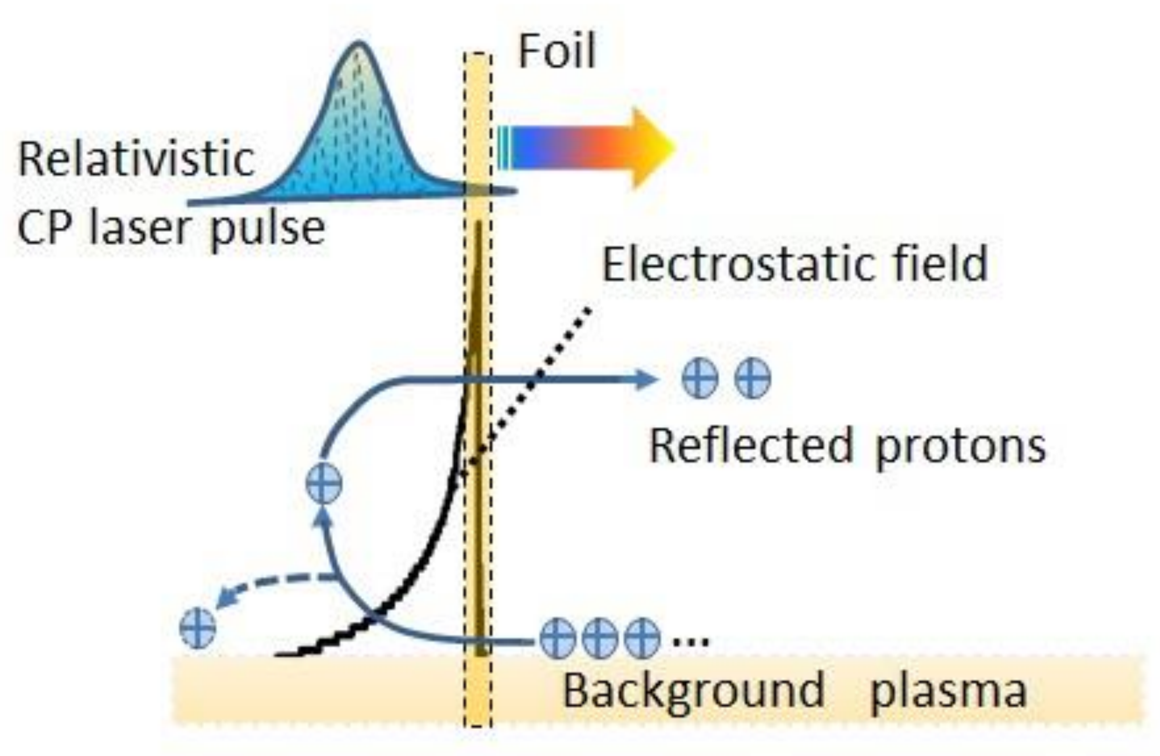

Lorentz boost

Reflected ions have 4γ more energy than the foil ions

Light Sail Drag Field Acceleration

Ji, Pukhov, Shen, *New Journal of Physics* ***16***, *063047* (2014)

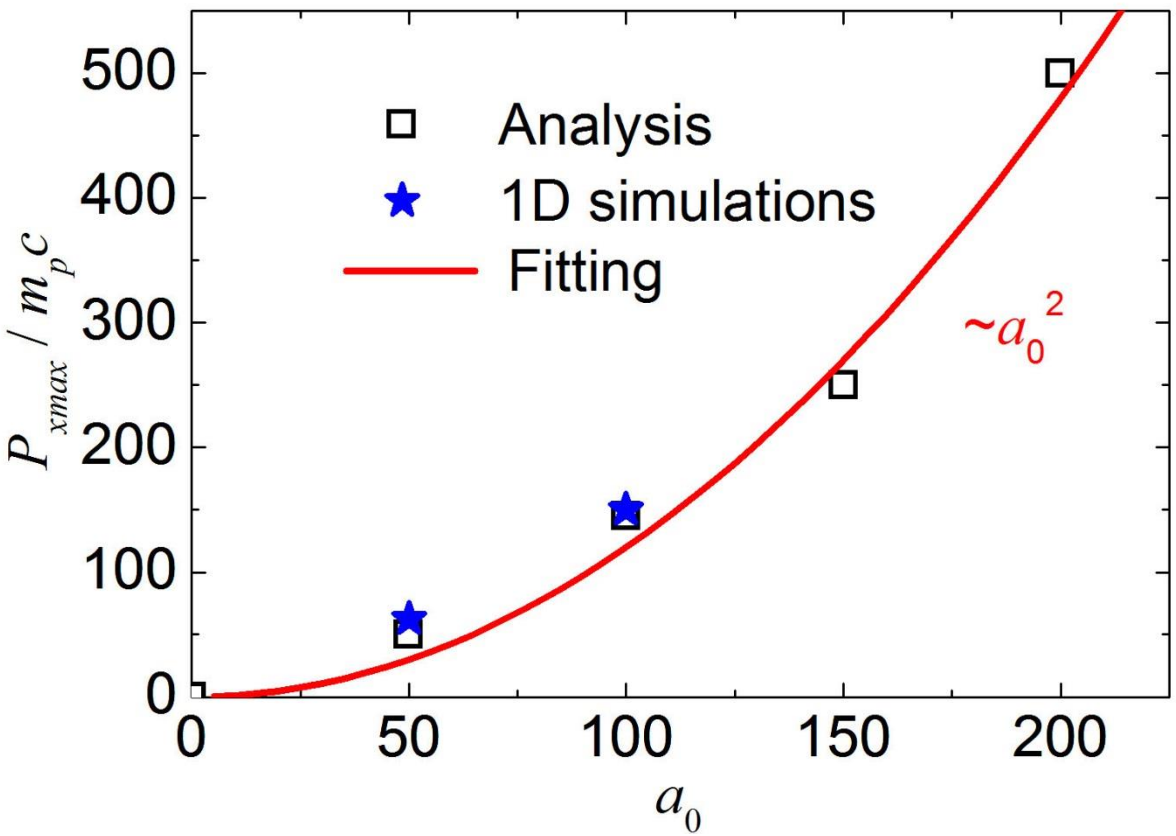

Light Sail Drag Field Acceleration

Ji, Pukhov, Shen, *New Journal of Physics* ***16***, *063047* (2014)

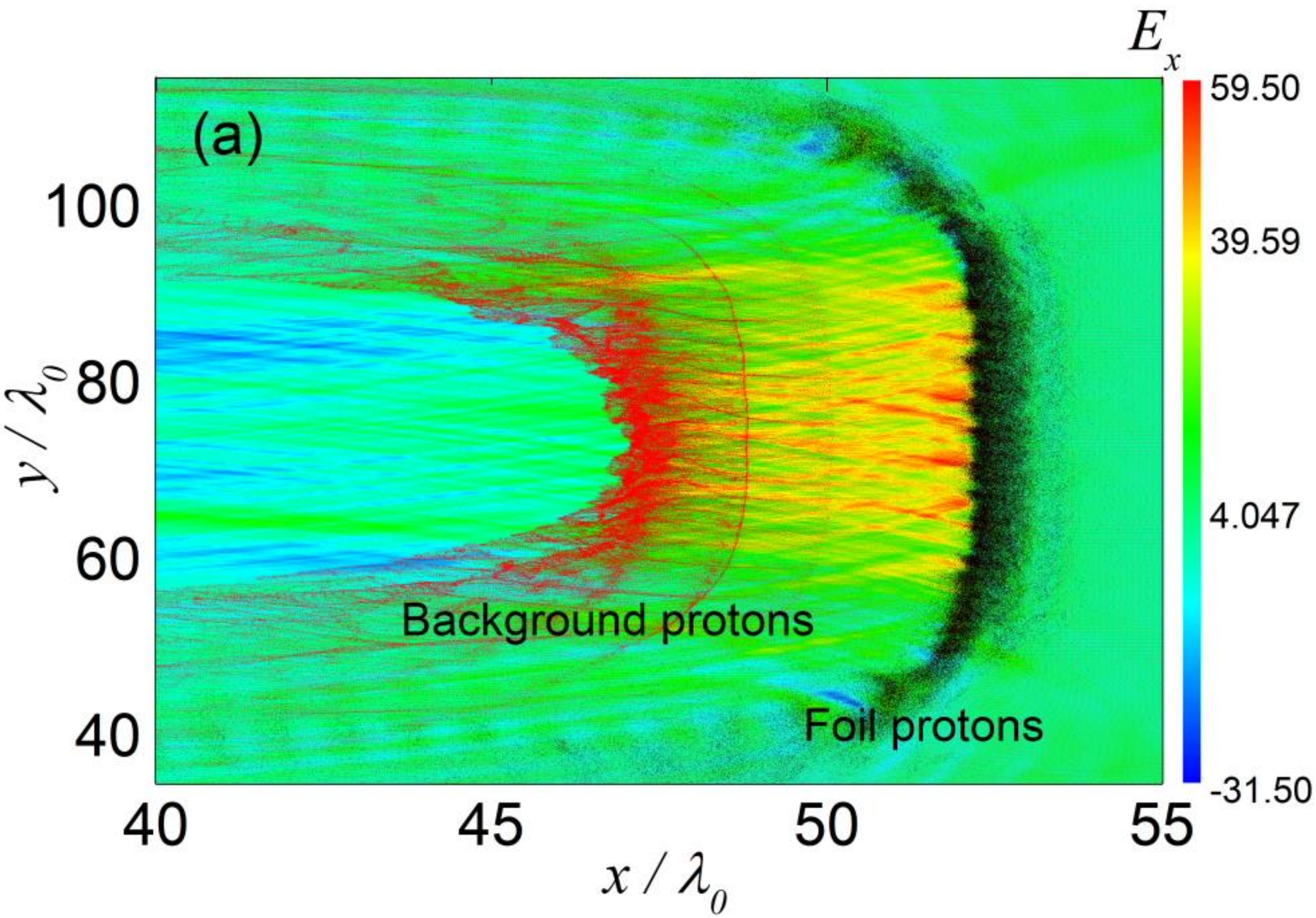

Light Sail Drag Field Acceleration

Ji, Pukhov, Shen, *New Journal of Physics* ***16***, *063047* (2014)

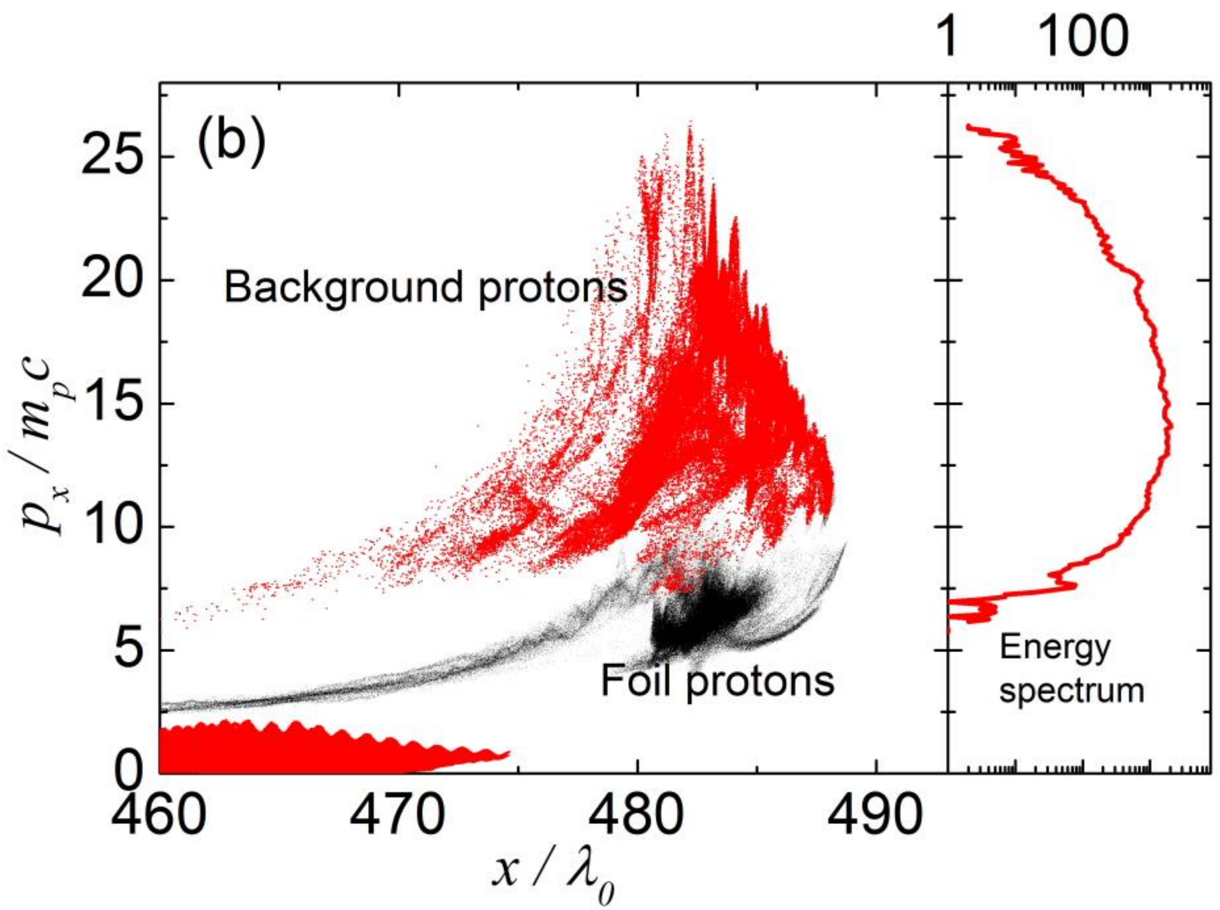

ELI, iZEST, iCAN, XCELS:

Laser-plasma interaction in the near-QED regime, I>10^{23} W/cm^2.

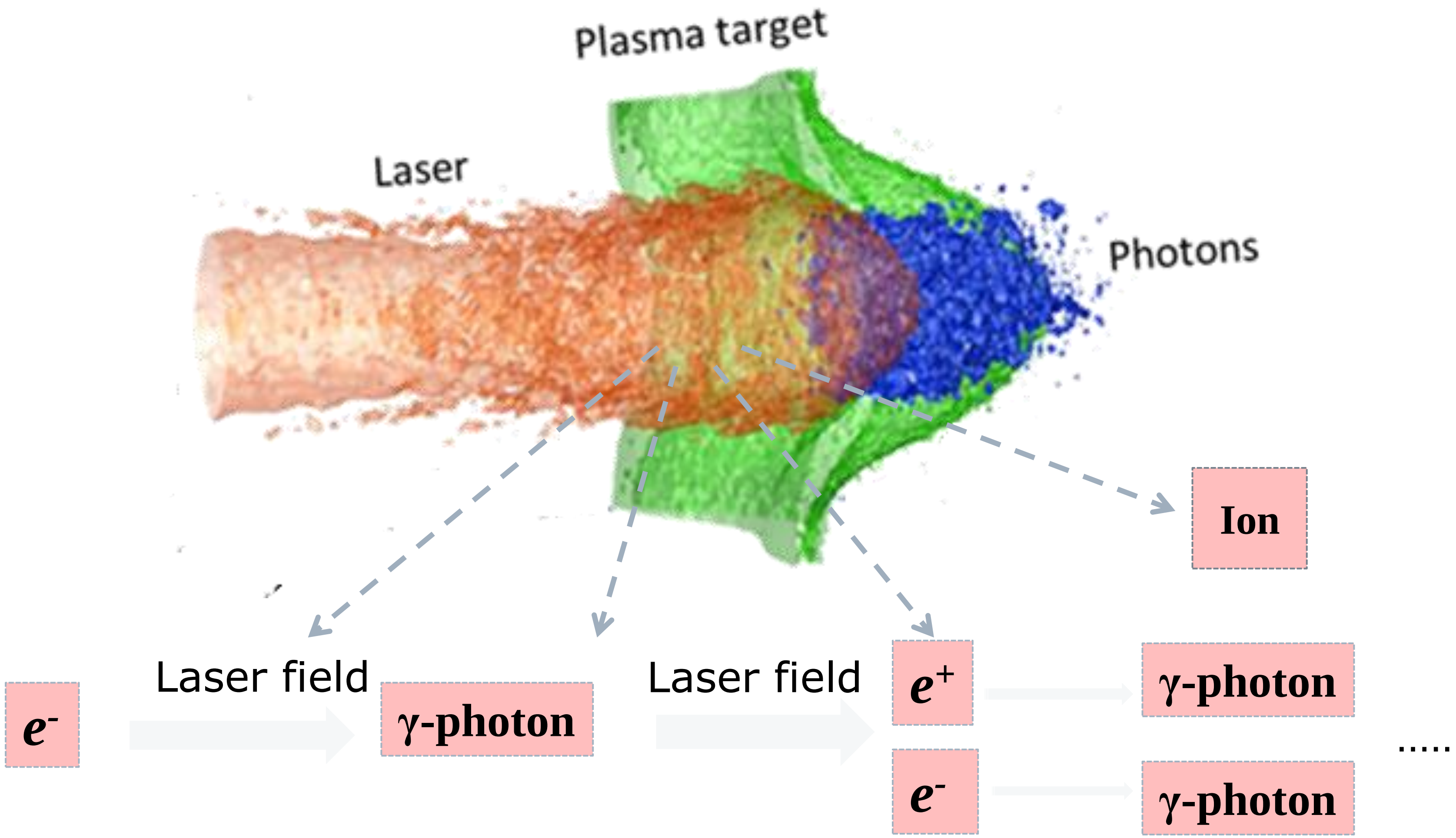

Relativistic Bremsstrahlung Classical Radiation Damping

The radiation reaction force F_R nearly equals Lorentz force F_L for a_0~300

$$\mathbf{F} = e\left(\mathbf{E} + \frac{1}{c}\mathbf{v}\times\mathbf{B}\right) + \mathbf{F}_R = \mathbf{F}_L + \mathbf{F}_R$$

$$\mathbf{F}_R = -\frac{2e^4}{3m^2c^4}\gamma^2\frac{\mathbf{v}}{c}\left[\left(\mathbf{E} + \frac{1}{c}\mathbf{v}\times\mathbf{B}\right)^2 - \frac{1}{c^2}(\mathbf{E}\mathbf{v})^2\right]$$

$$\left|\frac{\mathbf{F}_R}{\mathbf{F}_L}\right| = \frac{2}{3}k_0 r_e \gamma^2 \beta a_0$$

Nerush, Bashmakov, Kostyukov, *Phys. Plasmas* **18**, 083107 (2011)

HEINRICH HEINE UNIVERSITÄT DÜSSELDORF

Quantum Radiation Damping

The classical description fails when the photon energy becomes comparable with the electron energy

$$\frac{3}{2} a\gamma^2 \hbar\omega_0 > \gamma mc^2 \qquad \chi = \frac{\gamma E \sin\theta}{E_{crit}}$$

This happens for $a_0 > 400$

The maximum photon energy is limited at about $0.2\ \gamma mc^2$.

- The energy distribution of the probability rate for photon emission by relativistic charged particles in an electromagnetic field:

$$\frac{dW_{rad}(\varepsilon_\gamma)}{d\varepsilon_\gamma} = -\frac{\alpha m^2 c^4}{\hbar \varepsilon_e^2}\left\{\int_x^\infty Ai(\xi)d\xi + \left(\frac{2}{x} + \chi_\gamma\sqrt{x}\right)Ai'(x)\right\}$$

$$x = \left(\frac{\chi_\gamma}{\chi_e \chi_e'}\right)^{2/3} ;\chi_e' = \chi_e - \chi_\gamma \; (0 < \chi_\gamma < \chi_e)$$

$$W_{rad} \approx 1.46\frac{\alpha \mathrm{m}^2 c^4}{\hbar \varepsilon_e}\chi_e^{2/3} \quad \chi_e \gg 1$$

- The energy distribution of the probability rate for direct pair creation by hard photons:

$$\frac{dW_{cr}(\varepsilon_e)}{d\varepsilon_e} = \frac{\alpha m^2 c^4}{\hbar \varepsilon_\gamma^2}\left\{\int_x^\infty Ai(\xi)d\xi + \left(\frac{2}{x} - \chi_\gamma\sqrt{x}\right)Ai'(x)\right\}$$

$$\chi_e' = \chi_\gamma - \chi_e \; (0 < \chi_e < \chi_\gamma)$$

$$W_{cr} \approx 0.38\frac{\alpha m^2 c^4}{\hbar \varepsilon_\gamma}\chi_\gamma^{2/3} \quad \chi_\gamma \gg 1$$

$$W_{cr} \propto \exp\left(-\frac{8}{3\chi_\gamma}\right) \quad \chi_\gamma \ll 1$$

N. V. Elkina et al. Phys Rev. ST Accel . Beams 14, 054401 (2011)

QED in PIC: Monte-Carlo method

Two processes are included.

1. γ-photons emission in strong fields

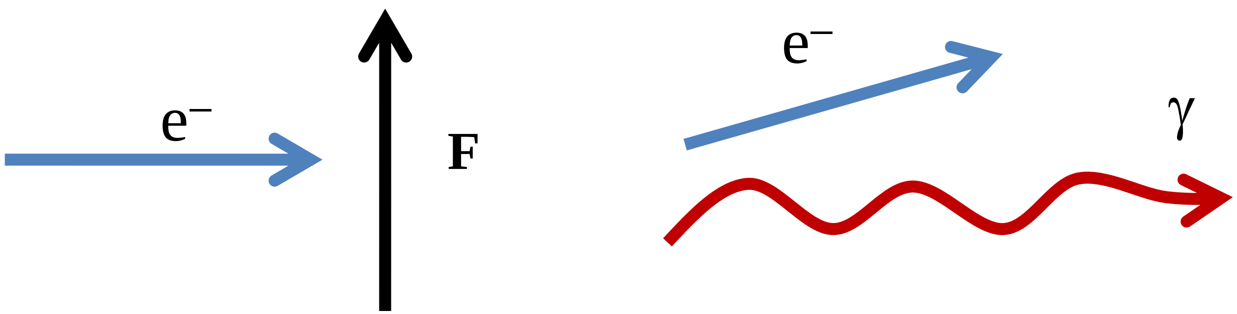

2. γ-photons decay in strong fields

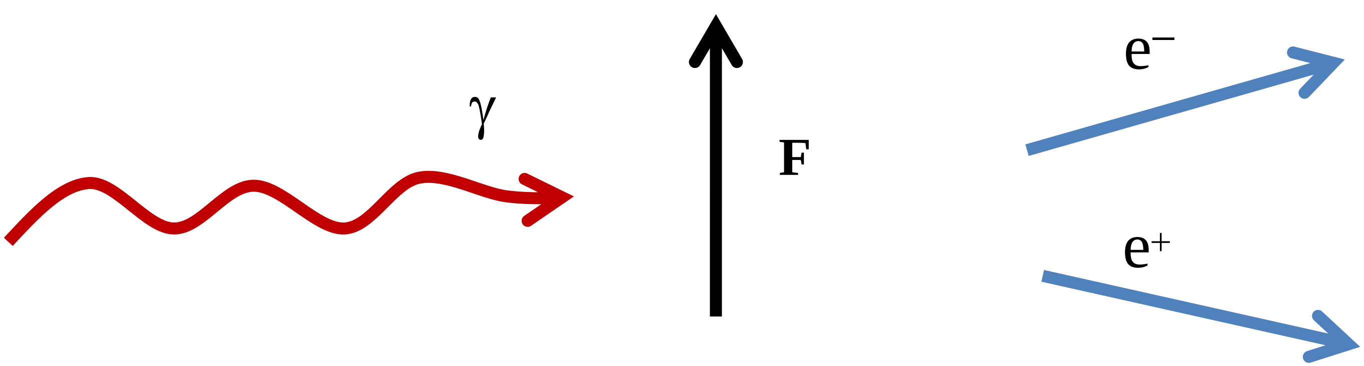

QED in VLPL: Monte-Carlo method

Example: GeV electron in $5 \cdot 10^4$ T magnetic field

γ-photons are tracked as particles in PIC

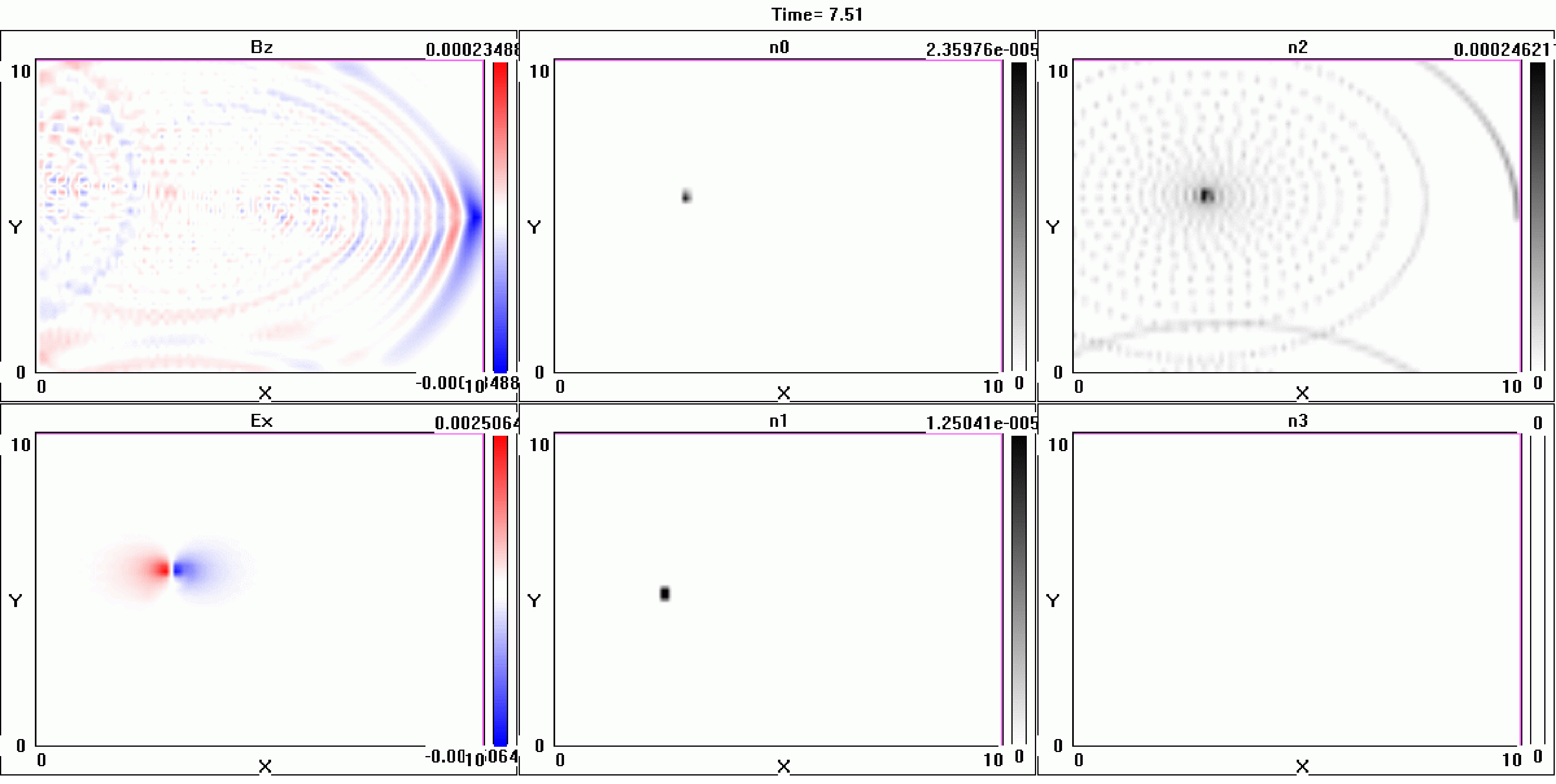

L. Ji et al, , *Phys. Plasmas* (2014)

Questions about near QED regime

- **How much energy goes to photons and positrons?**
- **With radiation reaction effect, how is the laser energy distributed between different species?**
- **Any unexpected phenomena?**

HEINRICH HEINE UNIVERSITÄT DÜSSELDORF

Simulation set up and parameters

Laser pulse duration: 54 fs, spot size: $r_0 = 4$ µm

Intensity: **3×10^{21} - 4×10^{24}** W/cm^2, linearly or circularly polarized

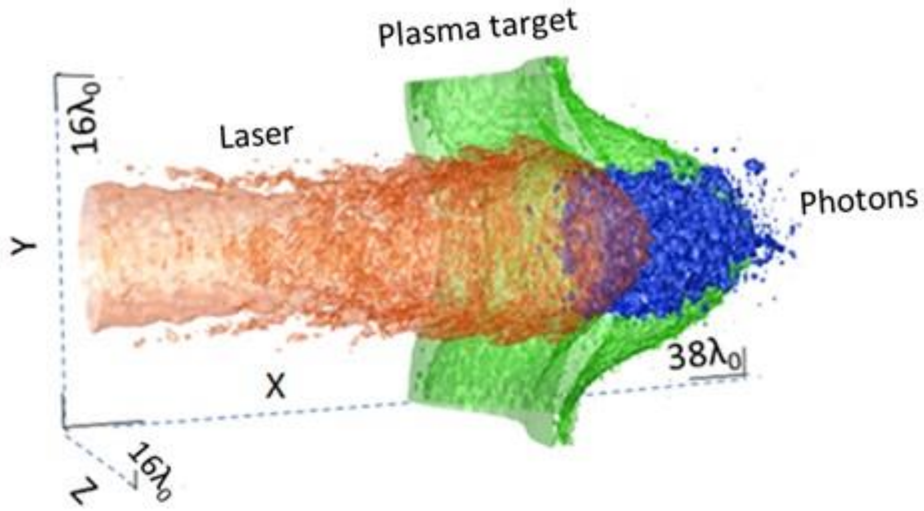

Bulk target: carbon (high density) or frozen hydrogen (low dense)

HEINRICH HEINE UNIVERSITÄT DÜSSELDORF

Energy absorption channels

Conversion efficiency for each plasma species as a function of laser intensity

- Electrons
- γ-photons
- Ions (protons or C)
- Positrons
- Total absorption efficiency

$$\eta_i \equiv E_{i,tot} / E_{Laser}$$

Carbon target: absorption channels

CP lasers

LP lasers

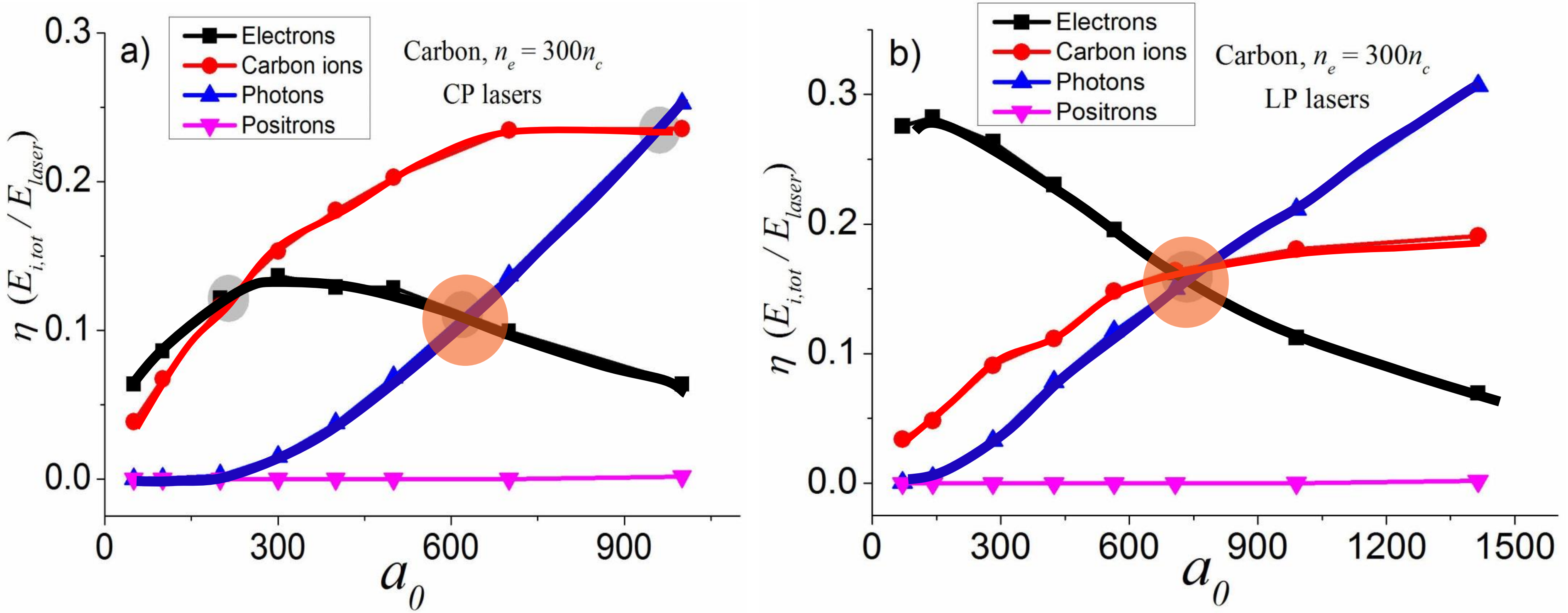

L. Ji et al, , *Phys. Plasmas* (2014)

Carbon target: power laws

$$\eta_{tot} = \eta_{e^- + c^{6+} + \gamma + e^+}$$

Power-laws converge at $I_0 > 10^{24}$ W/cm²

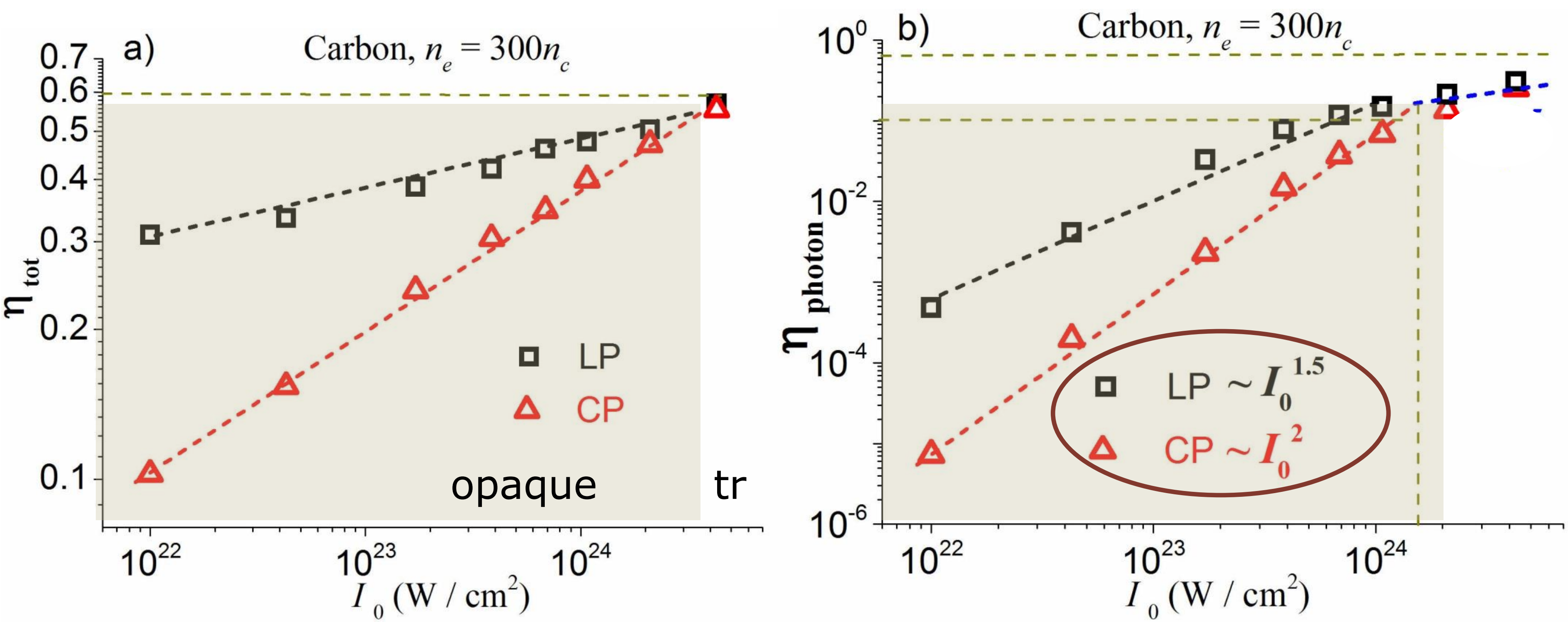

L. Ji et al, , *Phys. Plasmas* (2014)

Solid hydrogen target: energy absorption channels

CP lasers

LP lasers

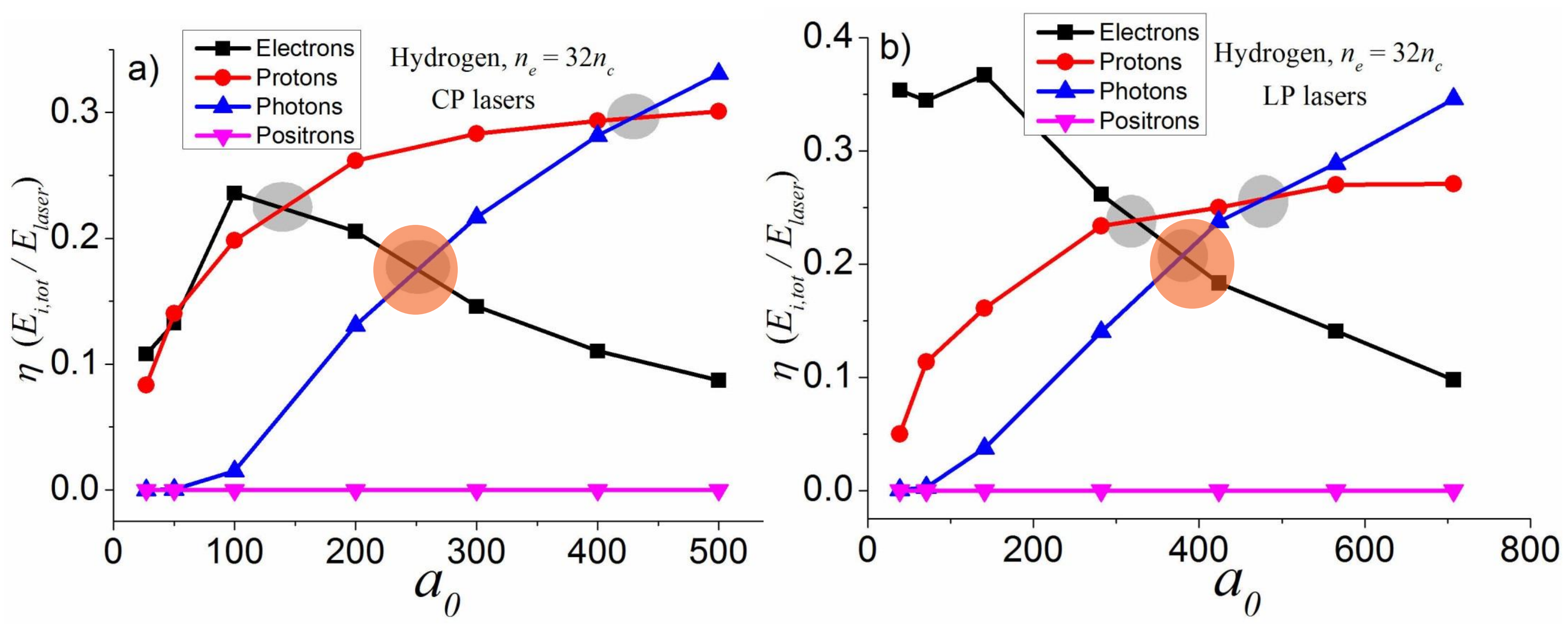

L. Ji et al, , *Phys. Plasmas* (2014),

Solid hydrogen target: power laws

$$\eta_{tot} = \eta_{e+p+\gamma+e^+}$$

Power-laws converge at $I_0 > 10^{23}$ W/cm²

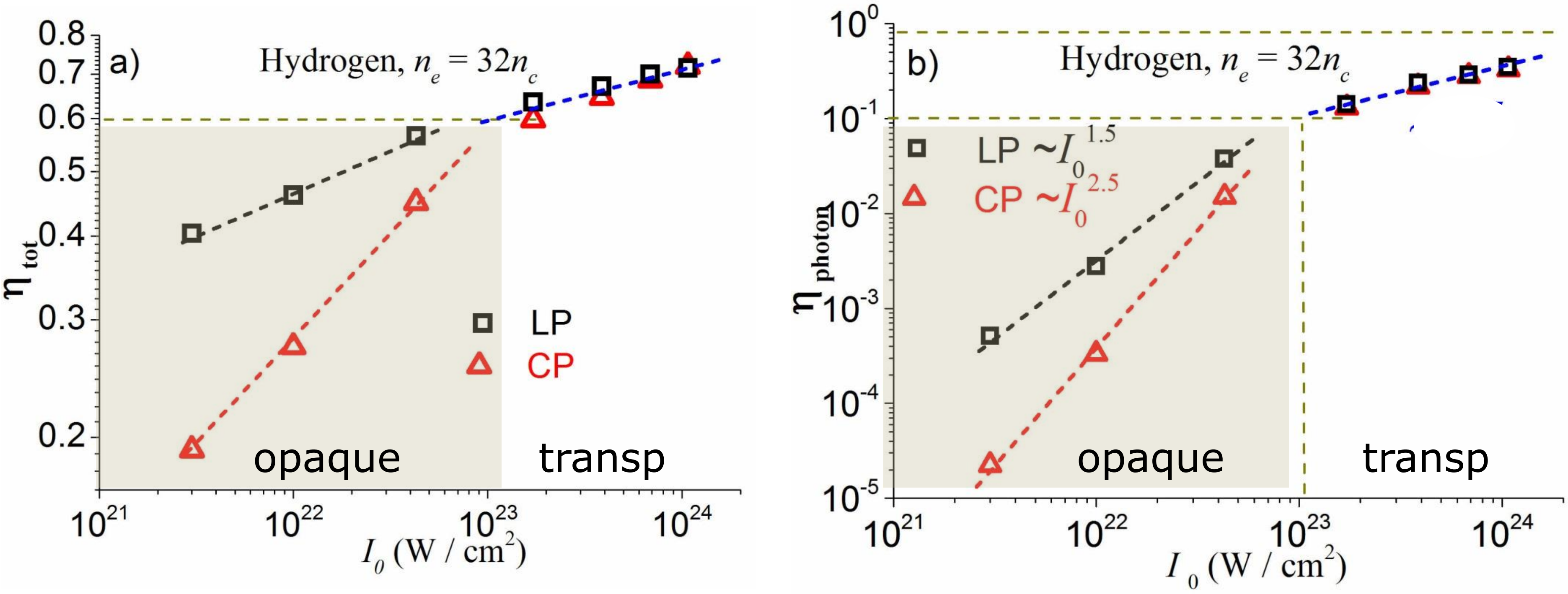

L. Ji et al, , *Phys. Plasmas* (2014)

HEINRICH HEINE UNIVERSITÄT DÜSSELDORF

Positrons

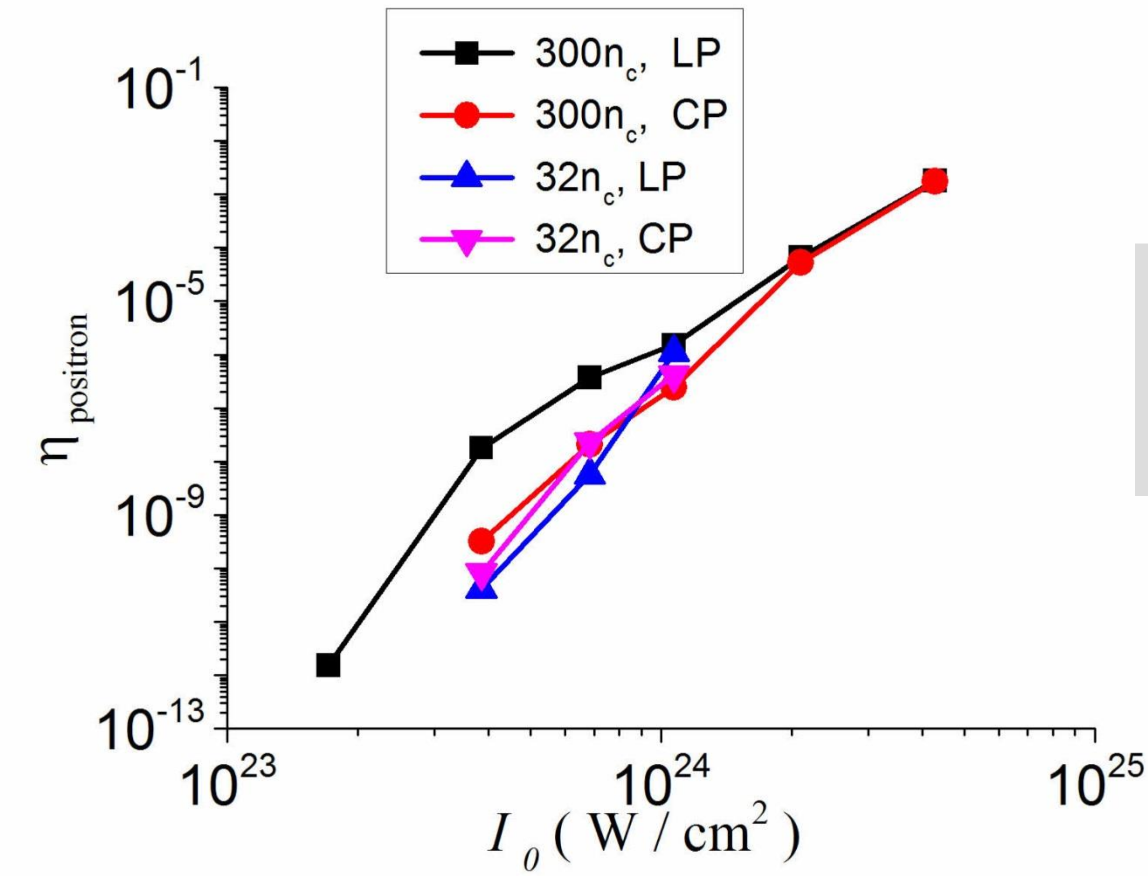

➢ Small below

$I_0 < 10^{25}$ W/cm^2

L. Ji et al, , *Phys. Plasmas* (2014)

Near-QED regime: plasma is an efficient γ-ray source

$\eta_{\gamma,\,max} \sim 35\%$

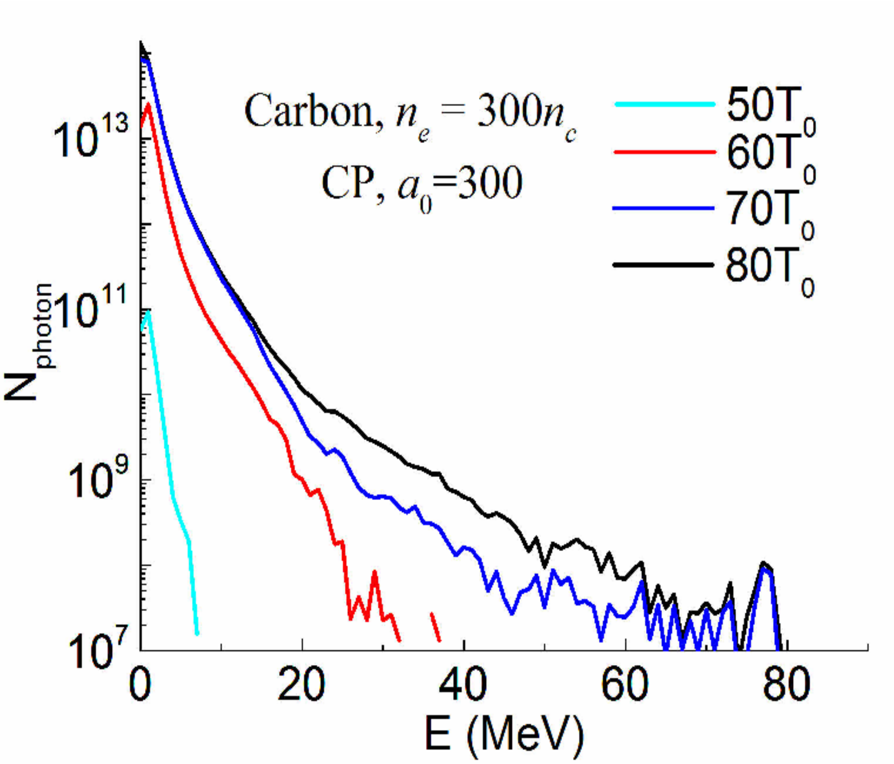

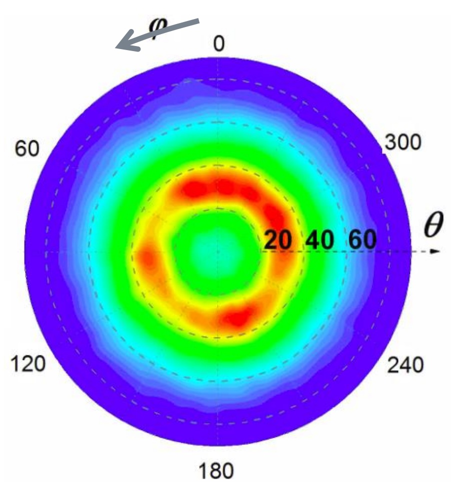

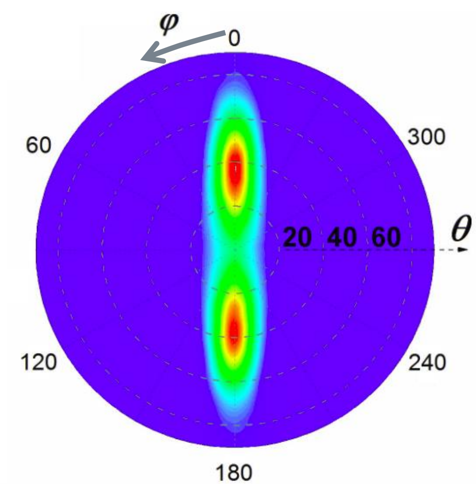

CP

LP

Radiation trapping of electrons in standing wave

Electron dynamics with radiation reaction

Radiation force, i.e. recoil at radiating hard photons at ultrarelativistic motion with acceleration, becomes of the order of the Lorentz force by the laser field. Particle trajectories acquire unusual properties that in turn results in new amazing gamma ray sources.

A. Gonoskov et al., arXiv: 1306.5734 [plasm-ph] PRL 2014

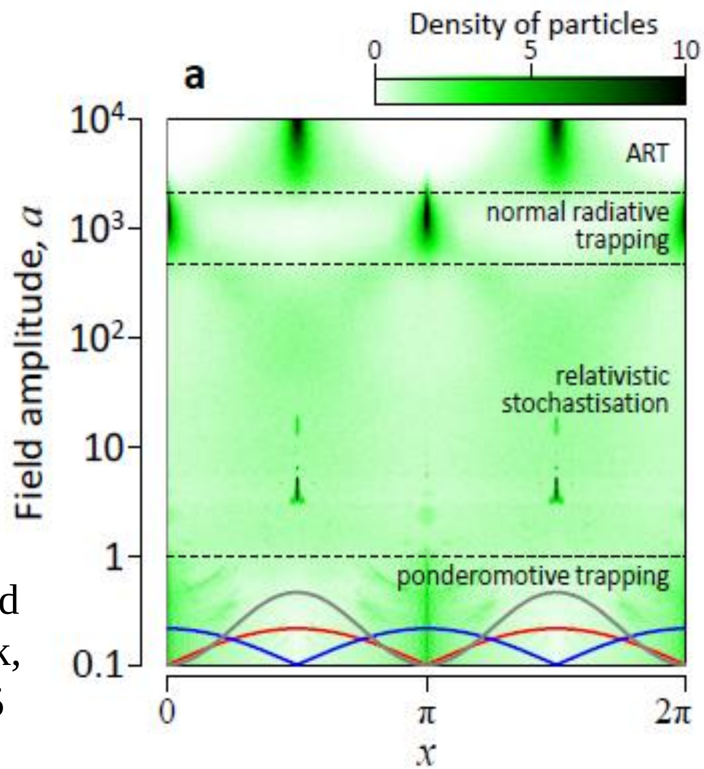

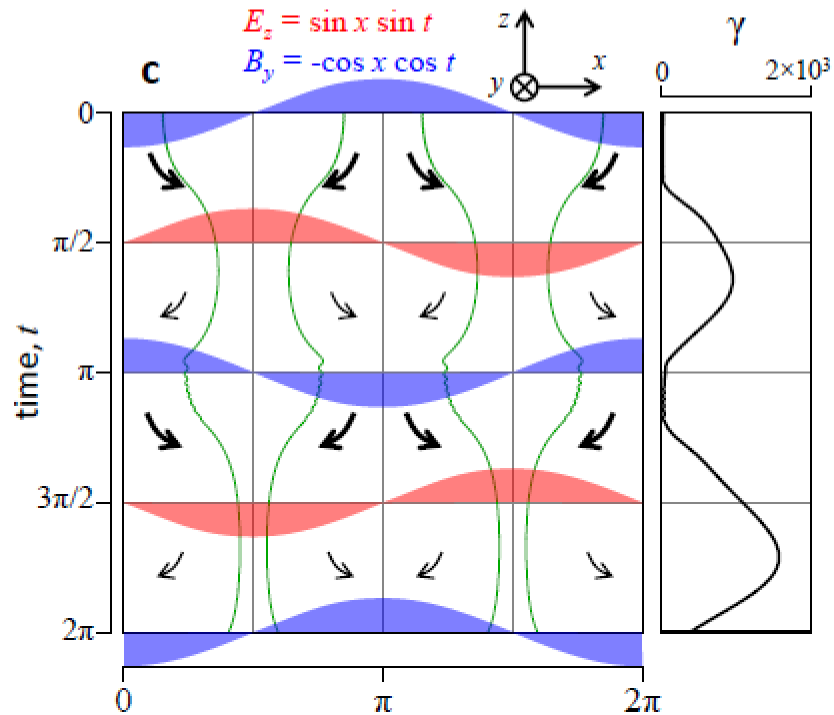

G. Lehmann and K. H. Spatschek, Phys. Rev. E 85 (2012) 056412

Phenomenon of radiative trapping: Electrons condense to minima (NRT) or or maxima (ART) of electric field

$$I_{th}^{NRT} \approx 5 \times 10^{23} \frac{W}{cm^2} \times \left(\frac{0.81\mu m}{\lambda}\right)^{\frac{4}{3}}$$

$$I_{th}^{ART} \approx 8 \times 10^{24} \frac{W}{cm^2} \times \left(\frac{0.81\mu m}{\lambda}\right)^{\frac{4}{3}}$$

Electron Trapping at Converging Dipole Wave Laser Focusing

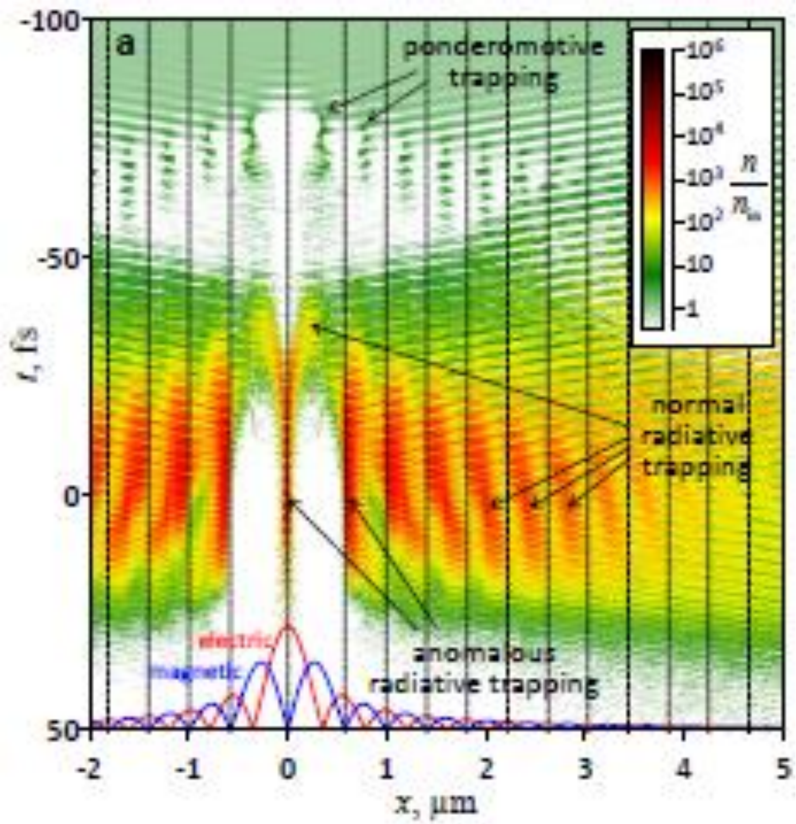

Electron density versus time and radius
at 30 fs dipole wave laser pulse focusing with peak
total power of 200 PW

A.V.Bashinov et al. Quantum Electronics 43(4),291 (2013),
A.Gonoskov et al. arXiv: 1306.5734 [plasm-ph], PRL 2014

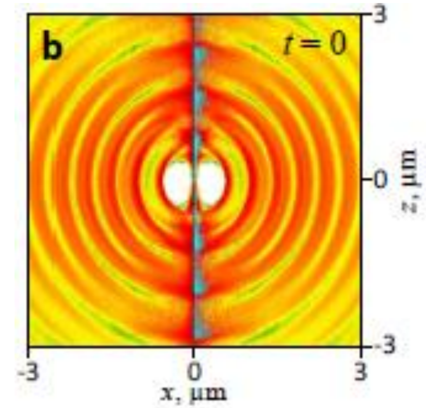

Density distribution at the instance of peak field strength; photons with energy exceeding 3 GeV are shown in cyan

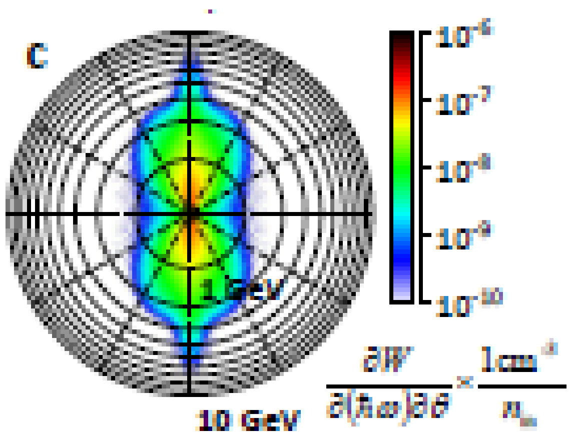

Hard photon emission distribution as a function of angle and energy (radial coordinate, log scale). 0.1% of laser energy is converted to > 1 GeV photons

Radiative trapping

L. Ji et al, PRL **112**, 145003 (2014)

Unexpected:
radiative trapping
in a plasma channel

L. Ji et al, PRL **112**, 145003 (2014)

Radiative trapping in a channel

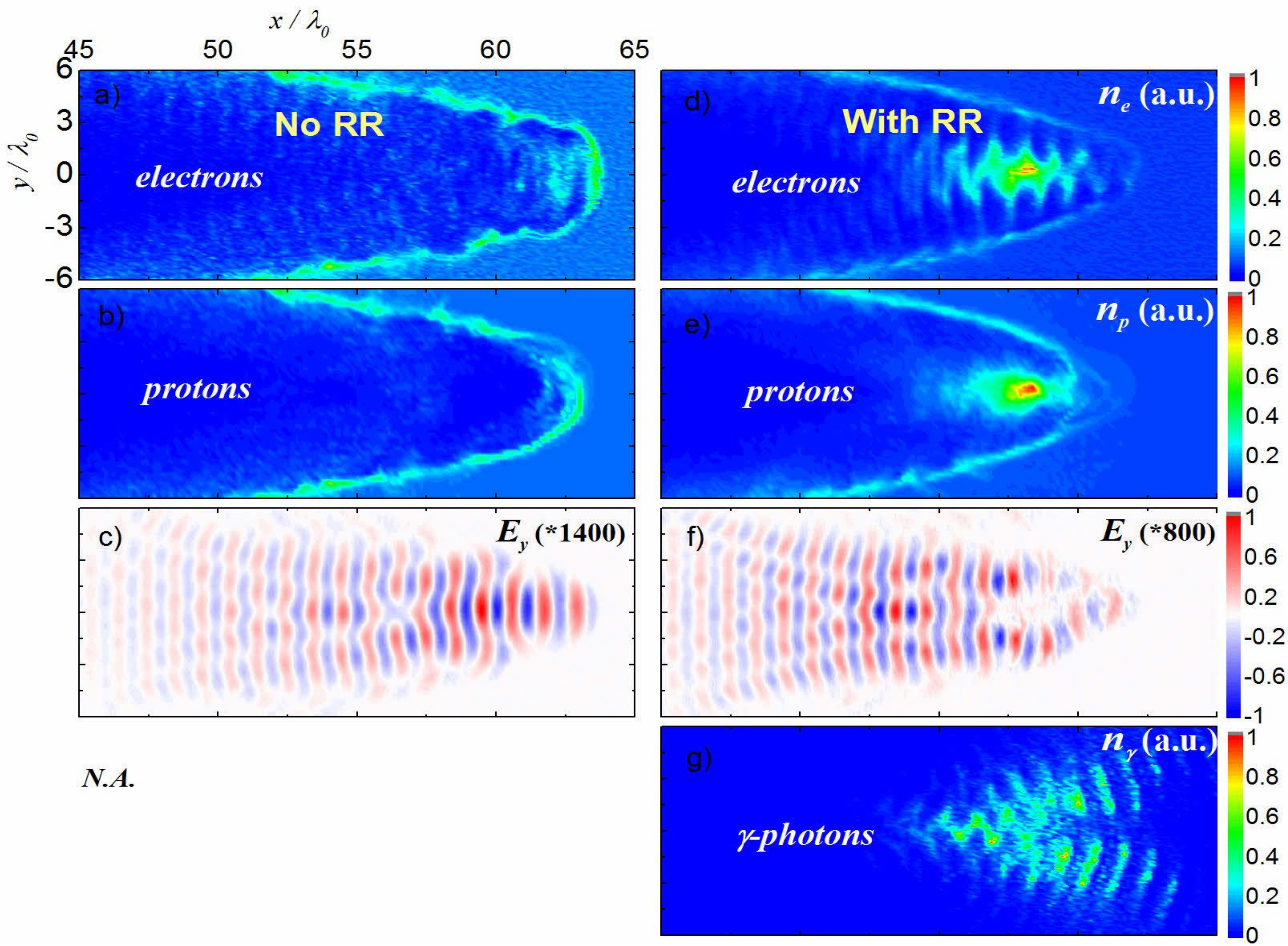

L. Ji et al, PRL **112**, 145003 (2014)

Physics of radiative trapping

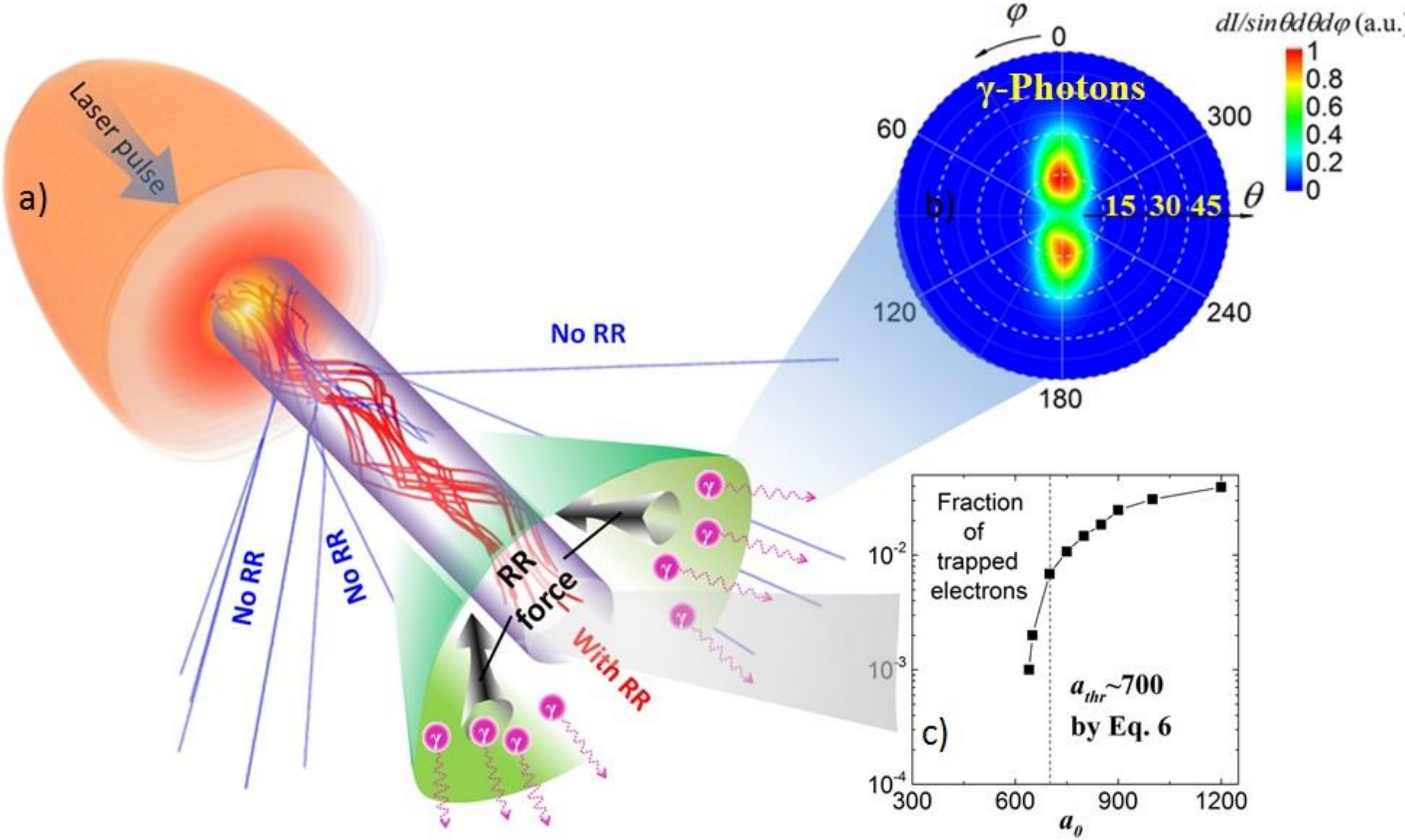

L. Ji et al, PRL **112**, 145003 (2014)

Radiation trapping: threshold behaviour

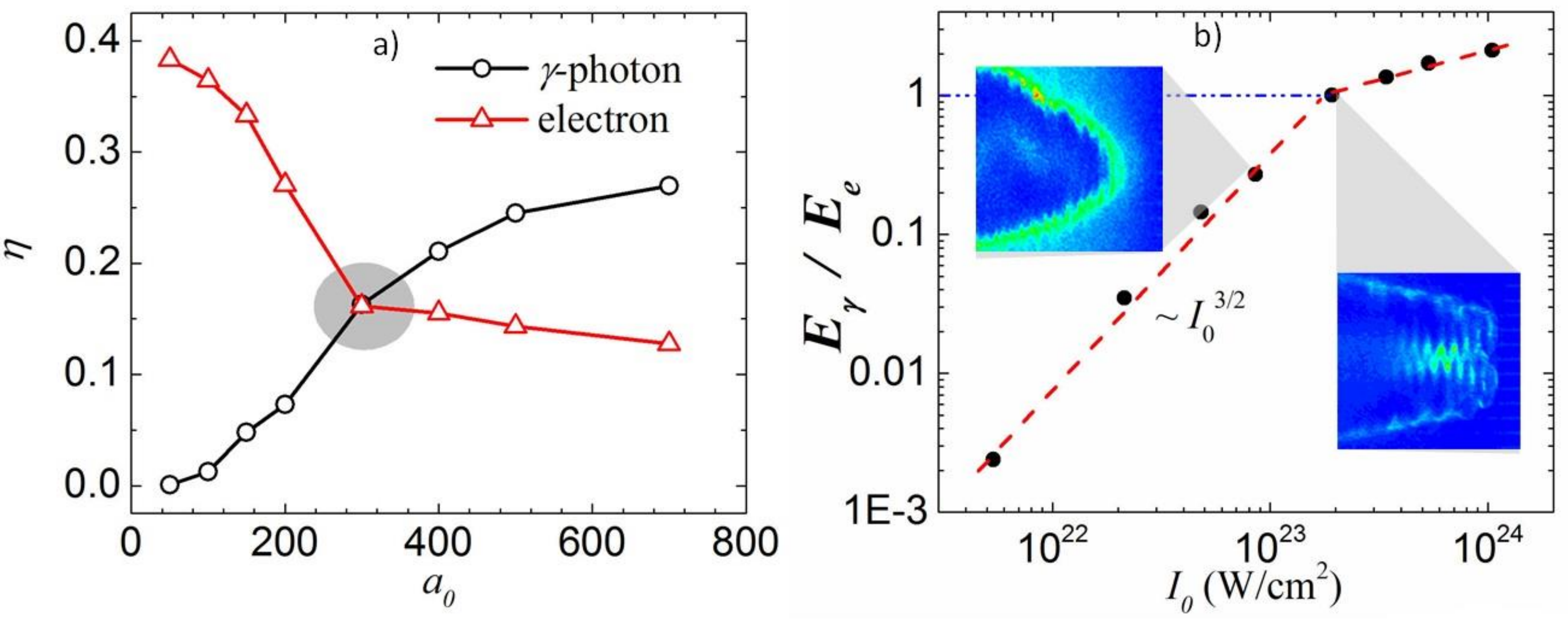

HEINRICH HEINE
UNIVERSITÄT DÜSSELDORF

Positron source with approachable lasers

a high-flux (6.8×10^{10}) dense (4×10^{22} cm^{-3}) GeV positron beam

$I_0 \approx 3 \times 10^{22}\ \mathrm{Wcm}^{-2}$

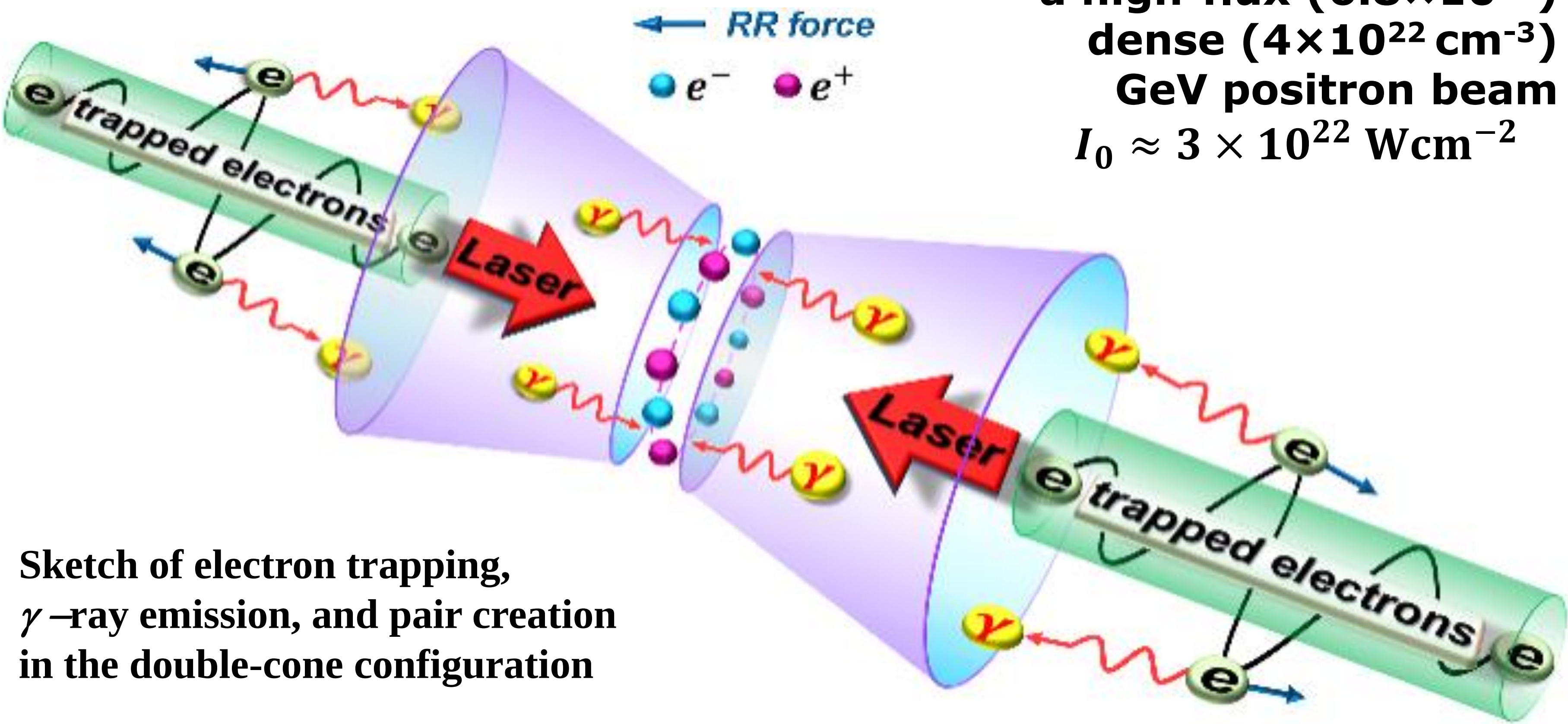

Sketch of electron trapping, γ–ray emission, and pair creation in the double-cone configuration

X. L. Zhu et al, submitted (2015)

Positron source with approachable lasers

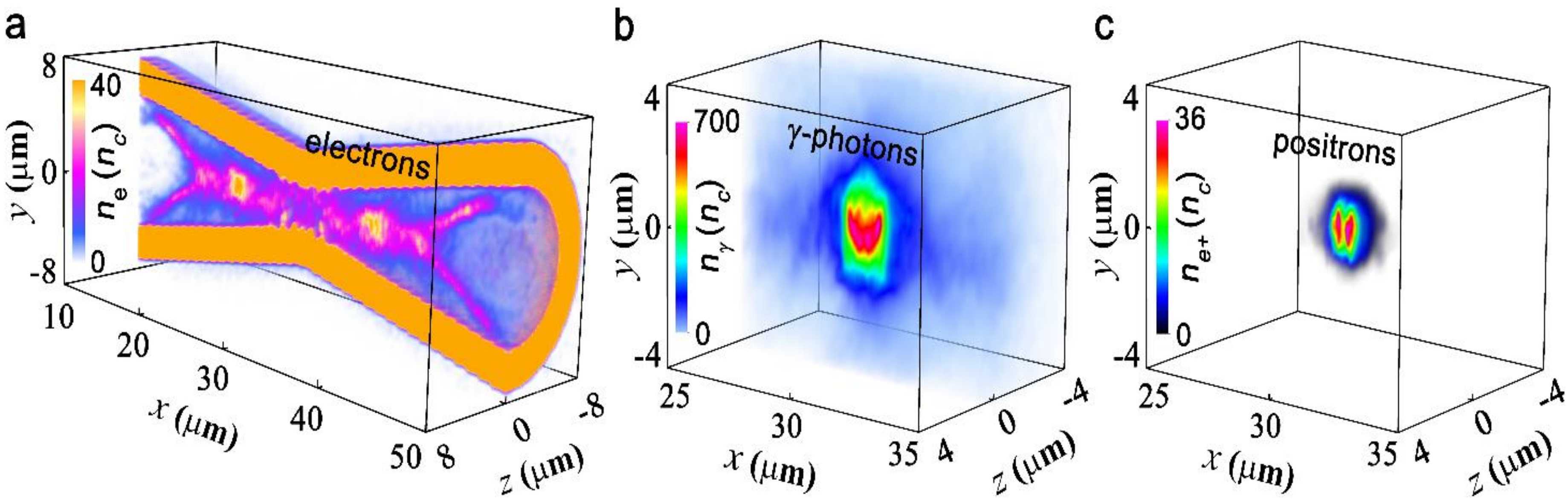

A dense electron bunch is formed in the cone.
The emitted photons have effective temperature of tens MeVs density up to 10^{24} cm^{-3}. Copious positrons are created in the cone with an density as high as $36n_c$.

X. L. Zhu et al, submitted (2015)

Positron source with approachable lasers

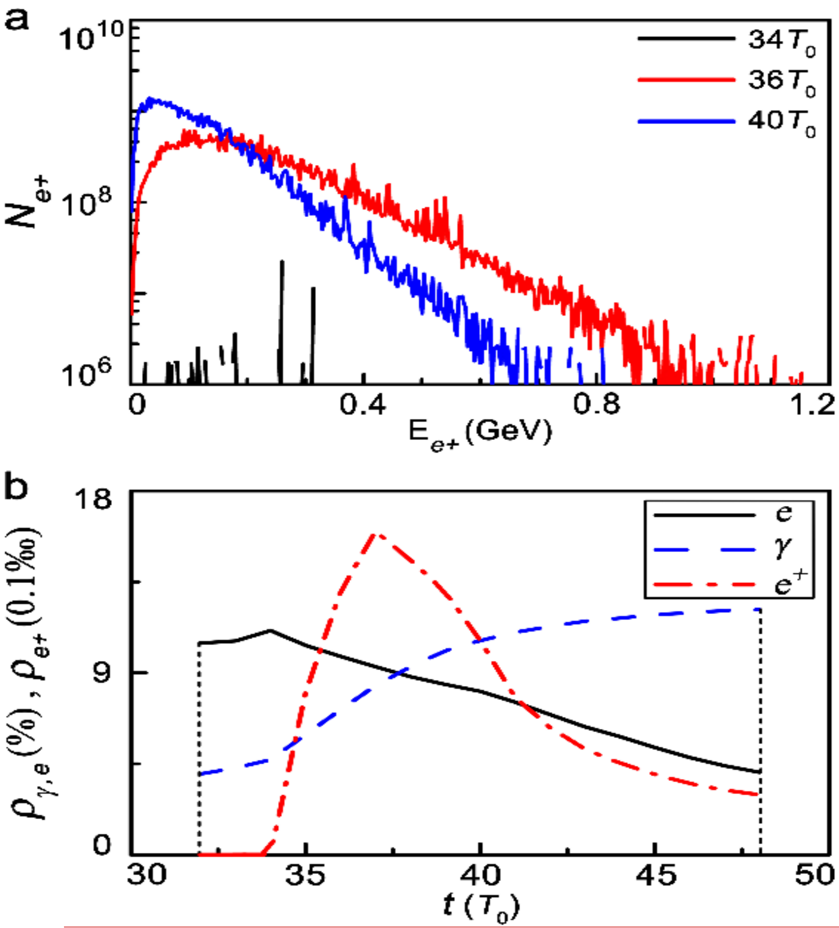

Evolution of positron energy spectra and laser energy conversion efficiency.

At $t=40T_0$, the positron energy decreases significantly because the positrons also emit photons and lose energy.

The electron energy increases at first, then decreases linearly by radiating photons, and is finally deposited in positrons and photons.

Positron source with approachable lasers

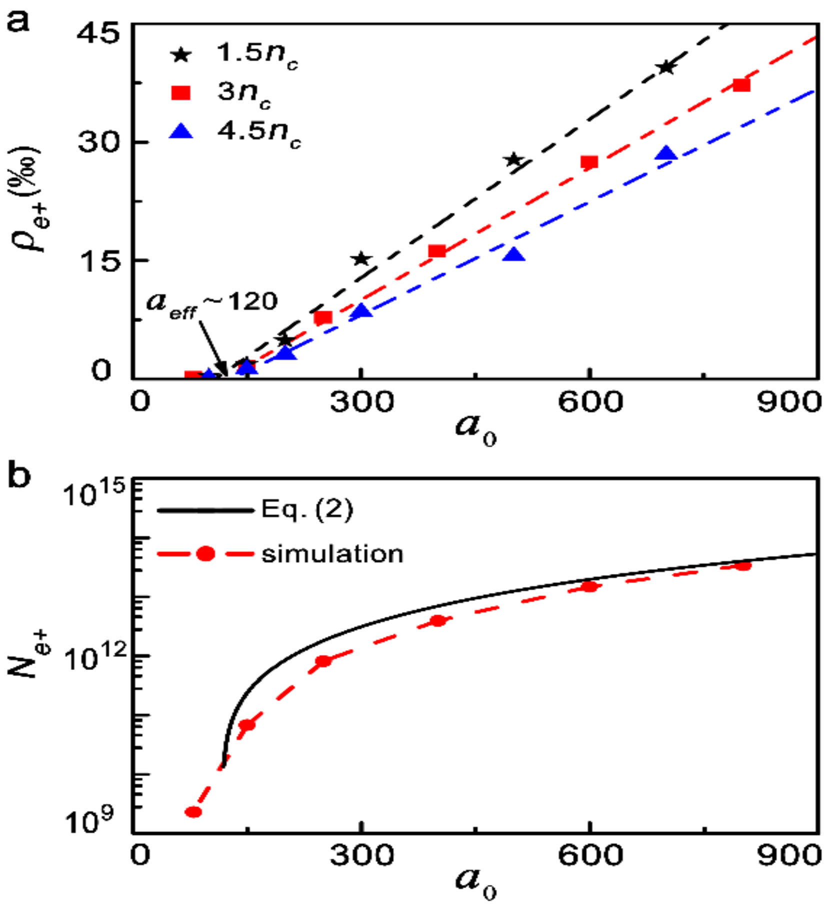

Results of theoretical predictions and simulations.

a, The laser energy conversion efficiencies to positrons with different laser intensities and NCD plasmas. There exists a laser threshold intensity, a_{eff}~120 for efficient positron production.

b, The positron yield based on analytics and PIC simulations.

X. L. Zhu et al, submitted (2015)

HEINRICH HEINE
UNIVERSITÄT DÜSSELDORF

Positron source with approachable lasers

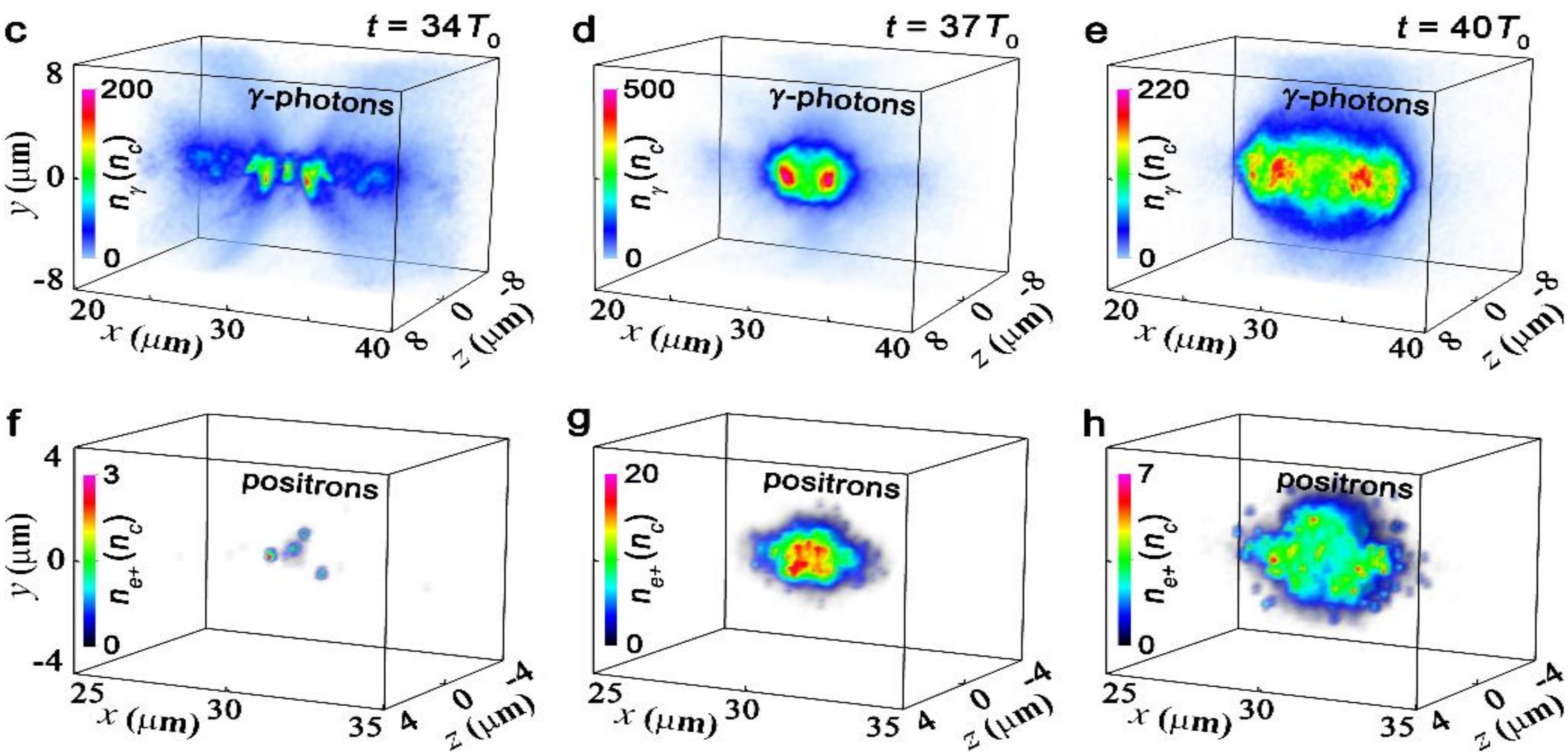

Density evolution of photons and positrons.

X. L. Zhu et al, submitted (2015)

HEINRICH HEINE UNIVERSITÄT DÜSSELDORF

Tunability of the positron source

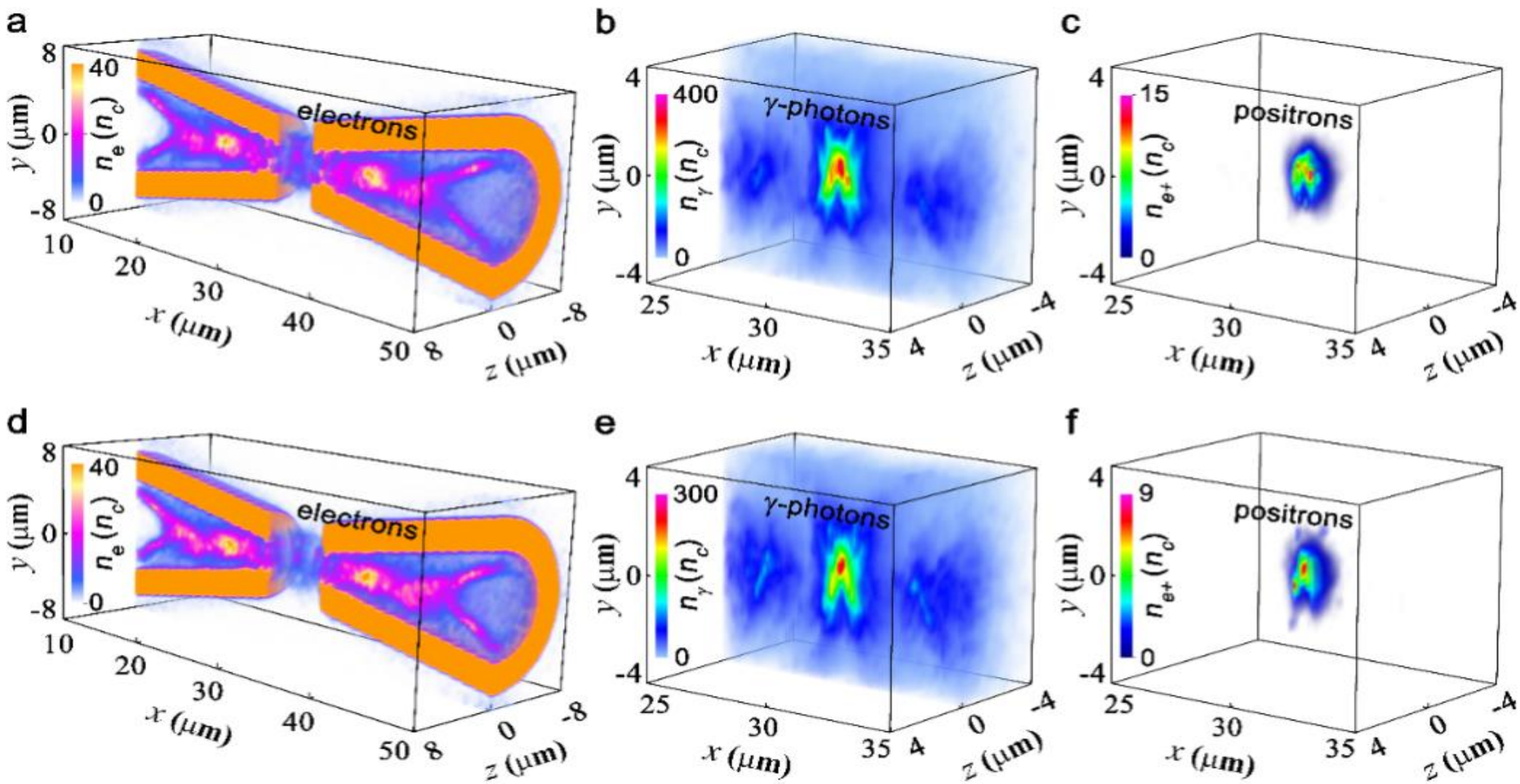

Simulation results with a short space between the double cones.

Summary

- Novel interaction physics in engineered targets
- 3D simulations of absorption channels

  in the near QED regime.
- Two interaction regions are distinguished:

  the opaque region and relativistic transparent region.
- Radiative trapping of electrons is revealed.
- Abundant positron source with next gen lasers